Modeling avian influenza using Filippov systems to determine culling of infected birds and quarantine

Nyuk Sian Chong [a,b], Robert J. Smith? [c,*]

[a] Department of Mathematics, The University of Ottawa, 585 King Edward Ave, Ottawa ON K1N 6N5, Canada
[b] School of Informatics & Applied Mathematics, Universiti Malaysia Terengganu, 21030 Kuala Terengganu, Malaysia
[c] Department of Mathematics and Faculty of Medicine, The University of Ottawa, 585 King Edward Ave, Ottawa ON K1N 6N5, Canada

ARTICLE INFO

ABSTRACT

The growing number of reported avian influenza cases has prompted awareness of the effectiveness of pharmaceutical or/and non-pharmaceutical interventions that aim to suppress the transmission rate. We propose two Filippov models with threshold policy: the avian-only model with culling of infected birds and the SIIR (Susceptible–Infected–Infected–Recovered) model with quarantine. The dynamical systems of these two models are governed by nonlinear ordinary differential equations with discontinuous right-hand sides. The solutions of these two models will converge to either one of the two endemic equilibria or the sliding equilibrium on the discontinuous surface. We prove that the avian-only model achieves global stability. Moreover, by choosing an appropriate quarantine threshold level I_c in the SIIR model, this model converges to an equilibrium in the region below I_c or a sliding equilibrium, suggesting the outbreak can be controlled. Therefore a well-defined threshold policy is important for us to combat the influenza outbreak efficiently.

1. Introduction

Recently, a new bird flu H7N9 has been reported as a threat to the public health across China. As an early stage of precaution, the China Health and Family Planning Commission has alerted the WHO (World Health Organization) about this infection [1,2]. Further, epidemiological investigations have been carried out to identify the root of the infection so that the disease can be controlled in the most effective and efficient way [2]. The public are also advised to take care of their personal hygiene, avoiding any contact with the sick or bird carcasses, reducing contact with wild birds and limiting unnecessary visits to poultry farms [3,2]. Humans can be infected by avian influenza through direct contact with dead or infected poultry and wild birds. People who have been infected by avian influenza may initially develop several symptoms such as fever, sore throat, muscle aches, cough, having breathing difficulties and conjunctivitis [4–6].

The spread of the new highly pathogenic avian influenza A viruses has not only triggered a major loss of life but has also cost a significant amount of money. Governments worldwide have spent billions of dollars to treat the infected patients and invest in prevention to control the disease [7]. Thus it is crucial to identify any possible effective control measures that

---

can eradicate the disease or at least to bring down the impact of the outbreak to a minimum level. That is, minimizing the number of infected is always a priority.

A significant number of mathematical modeling studies have been initiated to evaluate the effectiveness and the role of control measures in combating avian influenza [8–13]. Ferguson et al. [14] examined the effectiveness of targeted prophylaxis antiviral drug and social distancing measures in fighting an emerging influenza outbreak in Southeast Asia. Nuño et al. [15] assessed the basic public-health control strategies (such as using protective tools like gloves and masks, isolation in hospital wards and quarantine of suspected patients) in order to minimize the infection rate in hospitals and communities. The use of antiviral drugs and vaccination in combating a potential flu pandemic had also been discussed. Gulbudak and Martcheva [16] incorporated various approaches to culling of domestic birds: mass, modified and selective culling approaches. They concluded that, besides culling of domestic birds, timely employment of temporary control methods such as separation of poultry from wild birds, increasing biosecurity and prohibiting poultry movement and hatching eggs will either reduce the number of infected domestic birds or eradicate the disease in poultry.

Further, Agusto [17] applied optimal control theory to a system of ordinary differential equations to describe the transmission of two-strain avian influenza. Isolation of individuals with avian and mutant strains is represented by a pair of control variables. Moreover, cost-effectiveness of all possible combinations of the control measures is calculated. The results show that the combination strategy of isolating individuals with both avian and mutant strains is the most cost-effectiveness and provides more benefits towards disease eradication compared to only using one control strategy. Chong et al. [18] suggested that a combination of pharmaceutical (vaccination) and non-pharmaceutical (personal protection and isolation) interventions can combat avian influenza more effectively.

Several conventional control methods such as pharmaceutical or non-pharmaceutical interventions may be employed if the number of infected individuals exceeds a certain tolerant threshold, say I_c, in order to control or suppress the transmission rate of an emerging infectious disease. Thus, whenever the number of infected is below the threshold level I_c, the infection is considered tolerable. However, once the number of infected reaches I_c, we assume that an outbreak might occur. Henceforth, we call this type of disease management strategy a threshold policy [19–21].

Xiao et al. [22] extended the classical SIR model to a Filippov SIR model incorporating behavioral change of general individuals and implementation of necessary control measures by public authorities. They showed that the model solutions will either converge to one of the two endemic equilibria or the sliding equilibrium on the discontinuous surface. In order to preclude the outbreak or to stabilize the infection at a desired level, Xiao et al. suggested that choosing a proper combination of threshold level and control intensities is crucial.

Tang et al. [19] designed a piecewise HIV virus dynamic model with $CD4^+$ T cell counts to evaluate the strategies of structured treatment interruptions (STIs) of antiretroviral therapies. The dynamic models for drug-on and drug-off states with a single threshold and two thresholds (i.e., threshold window) are studied. Both models for STIs with single threshold and threshold window show that the $CD4^+$ T cell counts are preserved above a safe level. However, numerical results show that, by picking different lower and upper tolerant thresholds, it will either converge to a stable level or fluctuate. To conclude, an appropriate tolerant threshold of $CD4^+$ T cell counts and an individualized STI strategy based on the initial value of $CD4^+$ T cell counts for each individual patient are essential to compute the duration of drug on/off states for a patient.

In addition, Zhao et al. [23] proposed two Filippov plant disease models with cultural control strategy; a plant-disease model with replanting and roguing, and a Lotka–Volterra Filippov plant disease model with proportional planting rate. For the former model, a roguing rate that is proportional to the number of infected plants is considered. The global dynamic behavior of these models is discussed. Further, the global stability of five types of equilibria is thoroughly investigated.

An HPAI (highly pathogenic avian influenza) outbreak brings losses to the poultry business especially in commercialized poultry-processing industries. Besides the great loss in these business ventures, a significant number of birds will be destroyed [24,25]. The H5N1 outbreak in Hong Kong during 1997 caused an estimated loss of $13 million and the culling of 1.4 millions birds. In the 2001 H5N1 outbreak in Hong Kong, 1.2 million birds were killed, resulting in a total loss of $3.8 million. The H7N7 outbreak in 2003 in several European countries caused a loss of $314 million and 30 million birds [26,27].

HPAI viruses (H5 and H7 subtypes) usually cause infection among common bird species, such as chickens, ducks, pigeons, quails, turkeys and others. HPAI viruses can result in a very high mortality rate (90%–100%). Avian influenza viruses can be found mostly in the feces, saliva and nasal secretions of birds. Due to limited space of birds in the farm, avian influenza viruses can be spread easily among poultry flocks through aerosol or fecal-oral route [8,26,28]. Poultry, mainly chicken meat and eggs, are a valuable source of protein for many people, especially for lower-income groups, since chicken meat is the cheapest of all farm animals [29]. Hence, it is important for us to study avian influenza infections.

Here we would like to propose two mathematical models with piecewise control strategy that relate to threshold policy: an avian-only model with culling of infected birds as a control strategy in Section 2 and an SIIR model with quarantine as the control measure in Section 3. The dynamical systems of these two models are governed by nonlinear ordinary differential equations with discontinuous right-hand sides. The local asymptotic stability of disease-free and endemic equilibria in the regions below and above the threshold level are analyzed in each model. Further, the existence of a sliding mode, its dynamics and the global stability of the equilibria (if it exists) will also be investigated in each model. Finally, we will discuss the implications of our results in Section 4.

2. The avian-only model with culling of infected domestic birds

In this section, we consider an avian-only model incorporating culling of infected birds as a control strategy. Here we only consider domestic birds for the avian population. In order to manage the disease, the number of infected birds is used as an index of reference in applying the control strategy. The disease is considered to be manageable and the implementation of control methods is not required if the number of infected birds is below the tolerant threshold I_T. However, the action of culling the infected birds has to be employed immediately when the number of the infected birds exceeds the threshold level I_T. This action is essential to control the outbreak before the situation becomes more severe.

The avian-only model is driven by two compartments: susceptible domestic birds (S_d) and infected domestic birds (I_d). The total population of domestic birds, $N_d(t)$, is the sum of $S_d(t)$ and $I_d(t)$ at time t. Here, we represent the bird inflow, natural death and disease death by the parameters Λ_d, μ_d and d_d, respectively. The differential equations for this model are formulated as follows:

$$
\begin{aligned}
S_d'(t) &= \Lambda_d - \beta_d S_d I_d - \mu_d S_d \\
I_d'(t) &= \beta_d S_d I_d - (\mu_d + d_d) I_d - u_d c I_d
\end{aligned}
\tag{2.1}
$$

with

$$
u_d = \begin{cases} 0 & \text{for } I_d < I_T \Leftrightarrow \sigma_d(I_d) = I_d - I_T < 0 \\ 1 & \text{for } I_d > I_T \Leftrightarrow \sigma_d(I_d) = I_d - I_T > 0, \end{cases}
\tag{2.2}
$$

where $I_T > 0$ is the tolerance threshold, β_d is the rate at which domestic birds contract avian influenza and c is the culling rate of infected domestic birds.

Moreover, we divide $(S_d, I_d) \in \mathbb{R}_+^2$ into three regions as follows:

$$
\begin{aligned}
G_{1d} &:= \{(S_d, I_d) \in \mathbb{R}_+^2 ; I_d < I_T\} \\
G_{2d} &:= \{(S_d, I_d) \in \mathbb{R}_+^2 ; I_d > I_T\} \\
M_d &:= \{(S_d, I_d) \in \mathbb{R}_+^2 ; I_d = I_T\}.
\end{aligned}
$$

We define the normal vector perpendicular to M_d as $n_d = (0, 1)^T$ and the right-hand sides of (2.1) in region G_{id} are denoted by f_{id} for $i = 1, 2$, where

$$
f_{1d} = f_{1d}(S_d, I_d) = \begin{pmatrix} \Lambda_d - S_d(\beta_d I_d + \mu_d) \\ I_d \left[\beta_d S_d - (\mu_d + d_d)\right] \end{pmatrix}
$$

$$
f_{2d} = f_{2d}(S_d, I_d) = \begin{pmatrix} \Lambda_d - S_d(\beta_d I_d + \mu_d) \\ I_d \left[\beta_d S_d - (\mu_d + d_d + c)\right] \end{pmatrix}.
$$

Lemma 2.1. *The set $D_d = \left\{(S_d, I_d) \in \mathbb{R}_+^2 ; S_d + I_d \leq \frac{\Lambda_d}{\mu_d}\right\}$ is a positively invariant and attracting region for model (2.1) with any given initial conditions in $\mathbb{R}_+^2$.*

Proof. By adding both $S_d'(t)$ and $I_d'(t)$ of model (2.1), we get

$$
N_d' = \Lambda_d - \mu_d S_d - (\mu_d + d_d) I_d - u_d c I_d \leq \Lambda_d - \mu_d N_d.
\tag{2.3}
$$

Solving (2.3) by using an integrating factor, we obtain

$$
\begin{aligned}
\int_0^t \frac{d}{d\zeta}\left(N_d e^{\mu_d \zeta}\right) d\zeta &= \int_0^t \Lambda_d e^{\mu_d \zeta} d\zeta \\
N_d(t) e^{\mu_d t} &= N_d(0) + \frac{\Lambda_d}{\mu_d}\left(e^{\mu_d t} - 1\right) \\
N_d(t) &\leq \frac{\Lambda_d}{\mu_d} \quad \text{if } N_d(0) = S_d(0) + I_d(0) \leq \frac{\Lambda_d}{\mu_d}.
\end{aligned}
$$

Thus we obtain $N_d(t) \leq \frac{\Lambda_d}{\mu_d}$ if $N_d(0) \leq \frac{\Lambda_d}{\mu_d}$. Hence the region D_d is positively invariant.

Next, to show that D_d is an attracting region for model (2.1), let $N_d(t) > \frac{\Lambda_d}{\mu_d}$ and $\frac{\Lambda_d}{\mu_d} = \psi_d \implies \Lambda_d = \mu_d \psi_d$. From (2.3), we have

$$
N_d' \leq \Lambda_d - \mu_d N_d = \mu_d(\psi_d - N_d) < 0.
$$

We infer that the total population of domestic birds (i.e., $N_d = S_d + I_d$) of (2.1) is bounded by $\frac{\Lambda_d}{\mu_d}$. Moreover, every solution of model (2.1) with initial conditions in D_d will remain in D_d for $t > 0$. It is noteworthy to mention that every solution with initial conditions in $\mathbb{R}_+^2 \setminus D_d$ will approach D_d as $t \to \infty$. Hence the ω-limit sets of (2.1) are contained in D_d. ∎

Since D_d is a positively invariant and attracting region for model (2.1), the solution of model (2.1) exists in $D_d \forall t > 0$ and this model is mathematically and epidemiologically well-posed in D_d [30]. So it is sufficient to consider the dynamics of this model in D_d.

2.1. Analysis in region G_{1d}

In this section, we begin with the calculation of the basic reproduction number and then analyze the stability of the equilibria in region G_{1d}. The dynamics in region G_{1d} can be described by the following nonlinear ordinary differential equations:

$$\begin{pmatrix} S_d'(t) \\ I_d'(t) \end{pmatrix} = \begin{pmatrix} \Lambda_d - \beta_d S_d I_d - \mu_d S_d \\ \beta_d S_d I_d - (\mu_d + d_d) I_d \end{pmatrix} \equiv f_{1d}. \tag{2.4}$$

There are two equilibria involved in (2.4), the DFE (disease-free equilibrium), $E_{10d} = (S_d, I_d) = \left(\frac{\Lambda_d}{\mu_d}, 0 \right)$ and a unique positive EE (endemic equilibrium), $E_{11d} = \left(\frac{\mu_d + d_d}{\beta_d}, \frac{\Lambda_d \beta_d - \mu_d (\mu_d + d_d)}{\beta_d (\mu_d + d_d)} \right)$. The basic reproduction number (see [31,32] for further details) for model (2.4), R_{1d}, is given as follows:

$$R_{1d} = \frac{\Lambda_d \beta_d}{\mu_d (\mu_d + d_d)}.$$

In addition, we would like to show that the DFE and EE of model (2.4) achieve local asymptotic stability in the following theorems, and the Jacobian matrix for this model is

$$J_{1d}(S_d, I_d) = \begin{pmatrix} -\beta_d I_d - \mu_d & -\beta_d S_d \\ \beta_d I_d & \beta_d S_d - (\mu_d + d_d) \end{pmatrix}.$$

Theorem 2.2. *The DFE, E_{10d}, of model (2.4) is locally asymptotically stable if $R_{1d} < 1$.*

Proof. By solving the characteristic equation $|J_{1d}(E_{10d}) - \lambda I| = 0$, we obtain

$$(-\mu_d - \lambda)\left[\frac{\Lambda_d \beta_d}{\mu_d} - (\mu_d + d_d) - \lambda \right] = 0 \implies \lambda = -\mu_d < 0$$

$$\lambda = \frac{\Lambda_d \beta_d - \mu_d (\mu_d + d_d)}{\mu_d} < 0$$

if $R_{1d} < 1$. We conclude that, at the DFE, all eigenvalues of (2.4) are negative if $R_{1d} < 1$. Hence E_{10d} is locally asymptotically stable if $R_{1d} < 1$. ∎

Theorem 2.3. *The EE, E_{11d}, of model (2.4) is locally asymptotically stable if $R_{1d} > 1$.*

Proof. The eigenvalues of $J_{1d}(E_{11d})$ are

$$\lambda = \frac{1}{2} \left(-\frac{\Lambda_d \beta_d}{\mu_d + d_d} \pm \sqrt{\Delta_{1d}} \right) \quad \text{where } \Delta_{1d} = \left(\frac{\Lambda_d \beta_d}{\mu_d + d_d} \right)^2 - 4\left[\Lambda_d \beta_d - \mu_d (\mu_d + d_d) \right].$$

If $R_{1d} > 1$, we obtain $\Lambda_d \beta_d - \mu_d (\mu_d + d_d) > 0$. Thus all λ are complex eigenvalues with negative real parts if $\Delta_{1d} < 0$ since all associated parameters are positive. Otherwise, if $\Delta_{1d} > 0$, then $\Delta_{1d} < \left(\frac{\Lambda_d \beta_d}{\mu_d + d_d} \right)^2$, so all λ are negative real numbers.

It follows that E_{11d} is either a stable spiral or stable node. Hence E_{11d} achieves local asymptotic stability whenever $R_{1d} > 1$. ∎

2.2. Analysis in region G_{2d}

A similar analysis as shown in Section 2.1 will be carried out in this section. The following equations describe the dynamics in region G_{2d}.

$$\begin{pmatrix} S_d'(t) \\ I_d'(t) \end{pmatrix} = \begin{pmatrix} \Lambda_d - \beta_d S_d I_d - \mu_d S_d \\ \beta_d S_d I_d - (\mu_d + d_d + c) I_d \end{pmatrix} \equiv f_{2d}. \tag{2.5}$$

In G_{2d}, we found two equilibria: the DFE, $E_{20d} = (S_d, I_d) = \left(\frac{\Lambda_d}{\mu_d}, 0 \right)$, and a unique positive EE, $E_{21d} = \left(\frac{\mu_d + d_d + c}{\beta_d}, \frac{\Lambda_d \beta_d - \mu_d (\mu_d + d_d + c)}{\beta_d (\mu_d + d_d + c)} \right)$. Moreover, the basic reproduction number (refer to [31,32] for further details) for model (2.5), R_{2d}, is thus

$$R_{2d} = \frac{\Lambda_d \beta_d}{\mu_d (\mu_d + d_d + c)}.$$

Further, the local asymptotic stability of the DFE and EE of model (2.5) are shown in the following theorems.

Theorem 2.4. *The DFE E_{20d} of model* (2.5) *is locally asymptotically stable if* $R_{2d} < 1$.

We use a similar method as in the proof of Theorem 2.2 to demonstrate that all eigenvalues of (2.5) at E_{20d} are negative or have negative real parts whenever $R_{2d} < 1$. Therefore, we claim that E_{20d} is locally asymptotically stable if $R_{2d} < 1$.

Theorem 2.5. *The EE E_{21d} of model* (2.5) *is locally asymptotically stable if* $R_{2d} > 1$.

The same method as Theorem 2.3 can be used to prove Theorem 2.5, so we omit the proof here.

2.3. Existence of a sliding mode and its dynamics

Definition 2.1 ([23]). If $\langle n_d, f_{1d} \rangle > 0$ and $\langle n_d, f_{2d} \rangle < 0$ on $\Omega_d \subset M_d$, then Ω_d is the sliding region.

Types of regions on discontinuity surfaces are given in Appendix A.
   The existence of a sliding mode is assured if $\langle n_d, f_{1d} \rangle > 0$ and $\langle n_d, f_{2d} \rangle < 0$. In this case, we have

$$\langle n_d, f_{1d} \rangle > 0 \quad \text{if } S_d > h_{1d} \equiv \frac{\mu_d + d_d}{\beta_d} \quad \text{and} \quad \langle n_d, f_{2d} \rangle < 0 \quad \text{if } S_d < h_{2d} \equiv \frac{\mu_d + d_d + c}{\beta_d}.$$

Note that we have $h_{1d} < h_{2d}$ whenever $c > 0$. So the sliding domain $\Omega_d \subset M_d$ is defined as follows:

$$\Omega_d = \left\{ (S_d, I_d) \in M_d; \frac{\mu_d + d_d}{\beta_d} < S_d < \frac{\mu_d + d_d + c}{\beta_d} \right\} = \left\{ (S_d, I_d) \in M_d; h_{1d} < S_d < h_{2d} \right\}.$$

Next, we find the sliding mode equations using Filippov convex method [33,34], which is demonstrated as follows:

$$\begin{aligned} f_d &= \alpha f_{1d} + (1 - \alpha) f_{2d} \quad \text{where } f_d = \begin{pmatrix} S'_d(t) \\ I'_d(t) \end{pmatrix} \quad \text{and} \quad \alpha = \frac{\langle n_d, f_{2d} \rangle}{\langle n_d, f_{2d} - f_{1d} \rangle} \\ \therefore f_d &= \begin{pmatrix} S'_d(t) \\ I'_d(t) \end{pmatrix} = \begin{pmatrix} \Lambda_d - \beta_d S_d I_d - \mu_d S_d \\ 0 \end{pmatrix}. \end{aligned} \tag{2.6}$$

Since the sliding mode only exists on $\Omega_d \in M_d$ and there is no change of I_d with respect to time t, we can rewrite (2.6) on Ω_d in following manner.

$$S'_d(t) = \Lambda_d - \beta_d S_d I_T - \mu_d S_d. \tag{2.7}$$

The sliding equilibrium, $E_d = \left(\frac{\Lambda_d}{\beta_d I_T + \mu_d}, I_T \right)$, is a unique pseudoequilibrium (refer to Appendix B for further discussion of types of equilibrium points for a Filippov system) if

$$\frac{\mu_d + d_d}{\beta_d} < \frac{\Lambda_d}{\beta_d I_T + \mu_d} < \frac{\mu_d + d_d + c}{\beta_d}. \tag{2.8}$$

By manipulating (2.8), we infer that E_d lies on Ω_d if

$$h_{3d} \equiv \frac{\Lambda_d \beta_d - \mu_d(\mu_d + d_d + c)}{\beta_d(\mu_d + d_d + c)} < I_T < \frac{\Lambda_d \beta_d - \mu_d(\mu_d + d_d)}{\beta_d(\mu_d + d_d)} \equiv h_{4d}.$$

In conclusion, E_d is locally asymptotically stable on Ω_d since $\frac{\partial}{\partial S_d}(\Lambda_d - \beta_d S_d I_d - \mu_d S_d) = -\beta_d I_T - \mu_d < 0$ where $\mu_d, \beta_d, I_T > 0$; i.e., the eigenvalue of (2.7) is negative.

2.4. Global stability of the endemic equilibria

We divide $(S_d, I_d) \in \mathbb{R}^2_+$ into three regions, G_{1d}, M_d and G_{2d}. For each region, there exists equilibrium points, E_d, E_{11d} and E_{21d}, which are located in regions M_d, G_{1d} and G_{2d}, respectively. In this section, we represent E_d, E_{11d}, E_{21d} and the initial point in Figs. 2–6 by symbols $\circ$, $\bullet$, $\times$ and $\blacksquare$, respectively. Next, the stability of equilibria E_d, E_{11d} and E_{21d} is discussed in the following subsections and some numerical simulations have been shown to depict the stability of the equilibrium point. All parameters are given in Table 1, unless otherwise stated.

2.4.1. Case 1: E_{11d} and E_{21d} are virtual equilibria if $h_{3d} < I_T < h_{4d}$
Let us denote the virtual equilibria E_{11d} and E_{21d} as E^V_{11d} and E^V_{21d}. These two equilibria are located in regions G_{2d} and G_{1d}, respectively. In this case, we claim that $E_d \in \Omega_d \subset M_d$ is globally asymptotically stable if $h_{3d} < I_T < h_{4d}$ in the following theorem. So if a limit cycle does not exist in model (2.1), then our claim is valid.

Table 1
Avian-only model (2.1) parameters.

Parameter	Description	Sample value	Units	Reference
Λ_d	Bird inflow	$\frac{2060}{365}$	Individuals per day	[35]
μ_d	Natural death of birds	$\frac{1}{2 \times 365}$	per day	[36]
β_d	Rate at which birds contract avian influenza	0.4	per individual per day	[37]
d_d	Disease death rate due to avian influenza in birds	0.1	per day	[36]
c	Culling rate of infected birds	1.5	per day	Assumed

Theorem 2.6. $E_d \in \Omega_d \subset M_d$ *is globally asymptotically stable if* $h_{3d} < I_T < h_{4d}$.

Proof. Let $g_1 = \Lambda_d - \beta_d S_d I_d - \mu_d S_d$, $g_2 = \beta_d S_d I_d - (\mu_d + d_d) I_d$, $g_3 = \beta_d S_d I_d - (\mu_d + d_d + u_d c) I_d$ and $g_4 = \beta_d S_d I_d - (\mu_d + d_d + c) I_d$. Consider a Dulac function, $B(S_d, I_d) = \frac{1}{S_d I_d}$ for regions $I_d < I_T$ and $I_d > I_T$ where $I_T > 0$ and $(S_d, I_d) \in \mathbb{R}_+^2$.

For regions $I_d < I_T$ and $I_d > I_T$, we obtain

$$
\begin{aligned}
\frac{\partial (Bg_1)}{\partial S_d} + \frac{\partial (Bg_3)}{\partial I_d} &= \frac{\partial}{\partial S_d}\left(\frac{\Lambda_d}{S_d I_d} - \beta_d - \frac{\mu_d}{I_d} \right) + \frac{\partial}{\partial I_d}\left(\beta_d - \frac{\mu_d + d_d + u_d c}{S_d} \right) \\
&= -\frac{\Lambda_d}{S_d^2 I_d} \\
&< 0 \quad \forall (S_d, I_d) \in \mathbb{R}_+^2 \setminus M_d.
\end{aligned}
\tag{2.9}
$$

We refer to [22], which has demonstrated that Dulac's theorem (see Theorem C.3 in Appendix C for more details) can be used to prove the non-existence of a limit cycle for a discontinuous dynamical system. In this case, the dynamical system (2.1) with (2.2) is discontinuous at the line $I_d = I_T$ and (2.9) is satisfied for $I_d \neq I_T$. In order to show the non-existence of limit cycle Γ that surrounds the sliding equilibrium E_d, we have to show that $\iint_{G_{id}} \left[\frac{\partial (Bg_1)}{\partial S_d} + \frac{\partial (Bg_3)}{\partial I_d} \right] dS_d dI_d < 0$ for $i = 1, 2$, by Green's Theorem. We would like to show this by contradiction. Assume that there exists a limit cycle Γ that passes through the discontinuous manifold M_d containing E_d and the sliding domain Ω_d in its interior. Suppose this limit cycle Γ has period T and direction as shown in Fig. 1. Let us denote the intersection points of Γ and M_d (i.e., the line $I_d = I_T$) as P and Q, the intersection points of Γ and the line $I_d = I_T - \delta$ as $P_1 = P + a_1(\delta)$ and $Q_1 = Q - a_2(\delta)$, and the intersection points of Γ and the line $I_d = I_T + \delta$ as $P_2 = P + b_1(\delta)$ and $Q_2 = Q - b_2(\delta)$ where $\delta > 0$ is sufficiently small. Moreover, we assume that $a_1(\delta)$, $a_2(\delta)$, $b_1(\delta)$ and $b_2(\delta)$ are continuous with respect to δ and $\lim_{\delta \to 0} a_i(\delta) = \lim_{\delta \to 0} b_i(\delta) = 0$ for $i = 1, 2$ are satisfied. The region G_{1d} is bounded by Γ_1 and segment $P_1 Q_1$, whereas the region G_{2d} is bounded by Γ_2 and segment $P_2 Q_2$. Furthermore, the nonlinear ordinary differential equations in region G_{1d} are denoted by g_1 and g_2. Let ∂G_{1d} denote the boundary of G_{1d}. By Green's Theorem, we obtain the following:

$$
\begin{aligned}
\iint_{G_{1d}} \left[\frac{\partial (Bg_1)}{\partial S_d} + \frac{\partial (Bg_2)}{\partial I_d} \right] dS_d dI_d &= \iint_{G_{1d}} \frac{\partial (Bg_1)}{\partial S_d} dS_d dI_d + \iint_{G_{1d}} \frac{\partial (Bg_2)}{\partial I_d} dS_d dI_d \\
&= \oint_{\partial G_{1d}} (Bg_1) dI_d - \oint_{\partial G_{1d}} (Bg_2) dS_d \\
&= \int_{\Gamma_1} Bg_1 dI_d + \int_{\overrightarrow{Q_1 P_1}} Bg_1 dI_d - \left(\int_{\Gamma_1} Bg_2 dS_d + \int_{\overrightarrow{Q_1 P_1}} Bg_2 dS_d \right) \\
&= \int_{\Gamma_1} \left(Bg_1 \cdot g_2 - Bg_2 \cdot g_1 \right) dt - \int_{\overrightarrow{Q_1 P_1}} Bg_2 dS_d \\
&= -\int_{\overrightarrow{Q_1 P_1}} Bg_2 dS_d
\end{aligned}
\tag{2.10}
$$

where $\frac{dS_d}{dt} = g_1 \implies dS_d = g_1 dt$, $\frac{dI_d}{dt} = g_2 \implies dI_d = g_2 dt$ and there are no changes of I_d in the segment $P_1 Q_1 \implies \int_{\overrightarrow{Q_1 P_1}} Bg_1 dI_d = \int_{I_T - \delta}^{I_T - \delta} Bg_1 dI_d = 0$.

Similarly, in G_{2d} the dynamical system is represented by g_1 and g_4. By Green's Theorem, we have

$$
\iint_{G_{2d}} \left[\frac{\partial (Bg_1)}{\partial S_d} + \frac{\partial (Bg_4)}{\partial I_d} \right] dS_d dI_d = -\int_{\overrightarrow{P_2 Q_2}} Bg_4 dS_d.
\tag{2.11}
$$

Suppose $G_{20} \subset G_{2d}$. Let $\zeta = \iint_{G_{20}} \left[\frac{\partial (Bg_1)}{\partial S_d} + \frac{\partial (Bg_4)}{\partial I_d} \right] dS_d dI_d = \oint_{\partial G_{20}} \left(Bg_1 dI_d - Bg_4 dS_d \right) < 0$ from (2.9). Thus we have

$$
0 > \zeta > -\left(\int_{\overrightarrow{Q_1 P_1}} Bg_2 dS_d + \int_{\overrightarrow{P_2 Q_2}} Bg_4 dS_d \right).
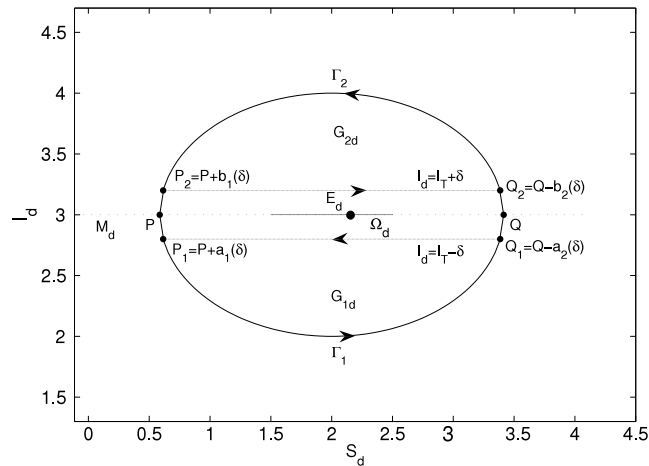\tag{2.12}
$$

Fig. 1. Limit cycle Γ.

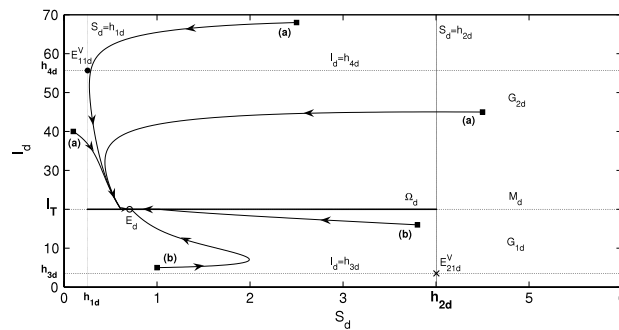**Fig. 2.** $E_d \in \Omega_d \subset M_d$ is globally asymptotically stable if $h_{3d} < I_T < h_{4d}$.

Moreover, by taking the limit $\delta \to 0$ of the addition of (2.10) and (2.11), we obtain

$$\lim_{\delta \to 0}\left(-\int_{\overrightarrow{Q_1P_1}} Bg_2 dS_d - \int_{\overrightarrow{P_2Q_2}} Bg_4 dS_d\right)$$
$$= \lim_{\delta \to 0}\left[\int_{P+a_1(\delta)}^{Q-a_2(\delta)}\left(\beta_d - \frac{\mu_d + d_d}{S_d}\right)dS_d - \int_{P+b_1(\delta)}^{Q-b_2(\delta)}\left(\beta_d - \frac{\mu_d + d_d + c}{S_d}\right)dS_d\right]$$
$$= \left[\beta_d S_d - (\mu_d + d_d)\ln S_d\right]_P^Q - \left[\beta_d S_d - (\mu_d + d_d + c)\ln S_d\right]_P^Q$$
$$= c(\ln Q - \ln P) > 0$$

since $Q > P$, which contradicts (2.12). Thus there are no limit cycles surrounding the sliding domain Ω_d and the sliding equilibrium E_d. Hence $E_d \in \Omega_d \subset M_d$ is globally asymptotically stable if $h_{3d} < I_T < h_{4d}$.　∎

Fig. 2 shows that all the trajectories with arbitrary initial conditions in $\mathbb{R}_+^2$ will converge to $E_d \in \Omega_d \subset M_d$ if $h_{3d} < I_T < h_{4d}$, as per Theorem 2.6. We pick $I_T = 20$ in this figure. Trajectories denoted by (a) will hit and slide to the right of Ω_d before converging to E_d. Meanwhile, trajectories (b) will hit and slide to the left of Ω_d and then move towards E_d.

Since $\frac{\Lambda_d}{\mu_d}$ (from Table 1) is large, it is unlikely we can show clearly that Case 1 will remain in the positively invariant and attracting region, $D_d = \left\{(S_d, I_d) \in \mathbb{R}_+^2; I_d + S_d \leq \frac{\Lambda_d}{\mu_d}\right\}$, as $t \to \infty$. For this reason, we increase μ_d to 0.3 in Fig. 3 to depict the convergence of solutions of Case 1 in region D_d and define $I_T = 8$. From Fig. 3, we found that the possible trajectories for this case are

(a) a trajectory that hits Ω_d from the region G_{1d} slides to the left of Ω_d and moves towards E_d.
(b) a trajectory with initial point located either inside or outside the attraction region D_d will cross M_d from G_{1d} to G_{2d}. Then the trajectory hits and slides to the left of Ω_d before converging to E_d.
(c) a trajectory with initial point located in G_{2d} either inside or outside of the attraction region D_d will hit and slide to the right of Ω_d before moving towards E_d.
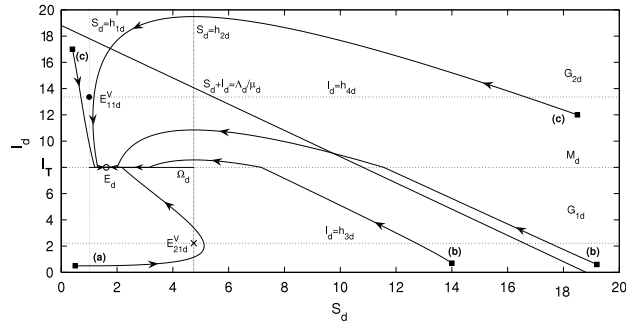
Fig. 3. All trajectories move towards $E_d \in \Omega_d \subset M_d$ in the positively invariant and attracting region $D_d = \left\{ (S_d, I_d) \in \mathbb{R}_+^2 \, ; \, I_d + S_d \leq \frac{\Lambda_d}{\mu_d} \right\}$ if $h_{3d} < I_T < h_{4d}$ is fulfilled.
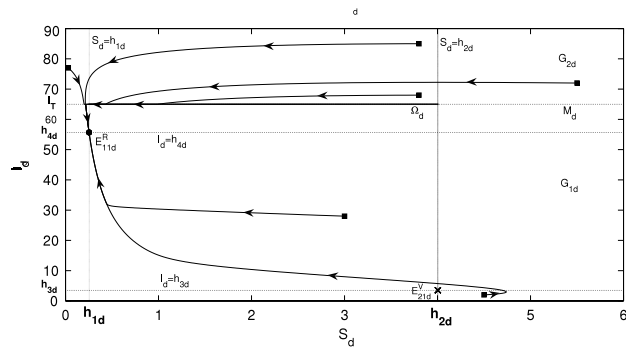

Fig. 4. $E_{11d}^R \in G_{1d}$ is globally asymptotically stable if $I_T > h_{4d}$.
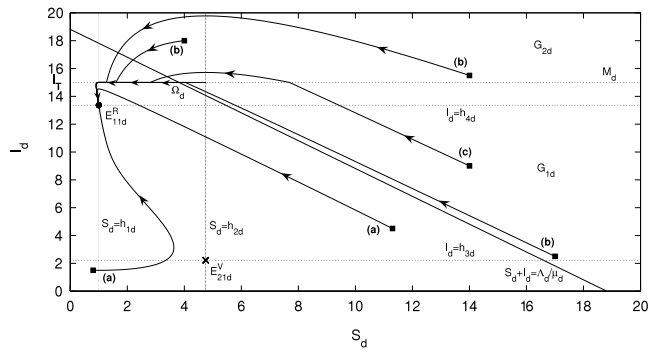

Fig. 5. All solutions of Case 2, where $I_T > h_{4d}$, will approach $E_{11d}^R \in G_{1d}$ in region $D_d = \left\{ (S_d, I_d) \in \mathbb{R}_+^2 \, ; \, I_d + S_d \leq \frac{\Lambda_d}{\mu_d} \right\}$ as $t \to \infty$.
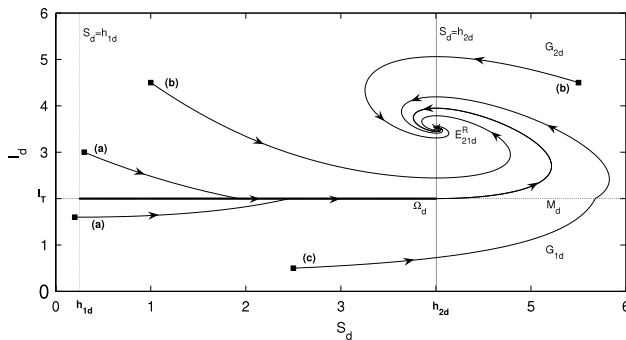

Fig. 6. $E_{21d}^R \in G_{2d}$ is globally asymptotically stable if $I_T < h_{3d}$.

2.4.2. Case 2: E_{11d} is a real equilibrium, whereas E_{21d} is a virtual equilibrium if $I_T > h_{4d}$

Let us denote E_{11d}^R as a real equilibrium and E_{21d}^V as a virtual equilibrium. Both of these equilibria are located in region G_{1d} and there is no equilibrium lying in region G_{2d}. Further, we claim that E_{11d}^R achieves global asymptotic stability if $I_T > h_{4d}$. In order to show the global behavior of E_{11d}^R in this case, we would like to consider the following Lyapunov functions for model (2.1), which have given rise to Theorem 2.7:

$$V_1 = V_1(S_d, I_d) = S_d - \frac{\mu_d + d_d}{\beta_d} - \frac{\mu_d + d_d}{\beta_d} \ln\left(\frac{\beta_d S_d}{\mu_d + d_d}\right) + I_d - \frac{\Lambda_d \beta_d - \mu_d(\mu_d + d_d)}{\beta_d(\mu_d + d_d)}$$
$$- \frac{\Lambda_d \beta_d - \mu_d(\mu_d + d_d)}{\beta_d(\mu_d + d_d)} \ln\left[\frac{\beta_d(\mu_d + d_d)I_d}{\Lambda_d \beta_d - \mu_d(\mu_d + d_d)}\right]$$

and

$$V_2 = V_2(S_d, I_d) = S_d - \frac{\mu_d + d_d + c}{\beta_d} - \frac{\mu_d + d_d + c}{\beta_d} \ln\left(\frac{\beta_d S_d}{\mu_d + d_d + c}\right) + I_d - \frac{\Lambda_d \beta_d - \mu_d(\mu_d + d_d + c)}{\beta_d(\mu_d + d_d + c)}$$
$$- \frac{\Lambda_d \beta_d - \mu_d(\mu_d + d_d + c)}{\beta_d(\mu_d + d_d + c)} \ln\left[\frac{\beta_d(\mu_d + d_d + c)I_d}{\Lambda_d \beta_d - \mu_d(\mu_d + d_d + c)}\right]. \tag{2.13}$$

Theorem 2.7. *The function*

$$V(S_d, I_d) = \begin{cases} V_1(S_d, I_d); & I_d < I_T \\ V_1(S_d, I_T) + V_2(S_d, I_d) - V_2(S_d, I_T); & I_d = I_T \text{ and } S_d \le \dfrac{\mu_d + d_d}{\beta_d} \\ V_1(S_d, I_T); & I_d = I_T \text{ and } S_d > \dfrac{\mu_d + d_d}{\beta_d} \\ V_1(S_d, I_d); & I_d > I_T \end{cases} \tag{2.14}$$

is a Lyapunov function on $\mathbb{R}_+^2$ for (2.1) and $\{E_{11d}^R\}$ is globally asymptotically stable if $I_T > h_{4d}$.

Proof. If $I_T > h_{4d}$, it follows that $\Lambda_d \beta_d < \beta_d(\mu_d + d_d)I_T + \mu_d(\mu_d + d_d) \Leftrightarrow \Lambda_d \beta_d < (\mu_d + d_d)(\beta_d I_T + \mu_d)$.

(a) We want to show that if $(S_d, I_d) \in G_{1d} := \{(S_d, I_d) \in \mathbb{R}_+^2; I_d < I_T\}$, then $\langle \nabla V, f_{1d} \rangle \le 0$.

In this particular case, we have the fact that $V_1(S_d, I_d) > 0 \forall (S_d, I_d) \in G_{1d}$ and $V_1(E_{11d}^R) = 0$. Then

$$\langle \nabla V, f_{1d} \rangle = \langle \nabla V_1, f_{1d} \rangle$$
$$= \frac{[\beta_d S_d - (\mu_d + d_d)][\Lambda_d - S_d(\beta_d I_d + \mu_d)]}{\beta_d S_d} + \frac{[(\mu_d + d_d)(\beta_d I_d + \mu_d) - \Lambda_d \beta_d][\beta_d S_d - (\mu_d + d_d)]}{\beta_d(\mu_d + d_d)}$$
$$= \frac{-\Lambda_d[\beta_d S_d - (\mu_d + d_d)]^2}{\beta_d S_d(\mu_d + d_d)}$$
$$\le 0 \quad \forall (S_d, I_d) \in G_{1d}$$

where $\langle \nabla V, f_{1d} \rangle = 0$ when $S_d = \frac{\mu_d + d_d}{\beta_d}$. Otherwise, $\langle \nabla V, f_{1d} \rangle < 0$.

(b) We claim that if $(S_d, I_d) \in \left\{(S_d, I_d) \in M_d; S_d \le \frac{\mu_d + d_d}{\beta_d}\right\}$ is satisfied, then we obtain $\sup_{0 \le \alpha \le 1} \langle \nabla V, \alpha f_{1d} + (1 - \alpha)f_{2d} \rangle = 0$.

For $I_d = I_T$ and $S_d \le \frac{\mu_d + d_d}{\beta_d}$, we have $V_1(S_d, I_T) + V_2(S_d, I_d) - V_2(S_d, I_T) > 0$. We find that, when $I_d = I_T$,

$$\langle \nabla V, f_{1d} \rangle = \frac{\Lambda_d[\beta_d S_d - (\mu_d + d_d)][(\mu_d + d_d + c) - \beta_d S_d]}{\beta_d S_d(\mu_d + d_d + c)} \le 0$$

where, for all $S_d \le \frac{\mu_d + d_d}{\beta_d}$, we have $\beta_d S_d - (\mu_d + d_d) \le 0$ and $(\mu_d + d_d + c) - \beta_d S_d > 0$. It follows that $\langle \nabla V, f_{1d} \rangle = 0$ when $S_d = \frac{\mu_d + d_d}{\beta_d}$. Otherwise, $\langle \nabla V, f_{1d} \rangle < 0$.

Again, we compute

$$\langle \nabla V, f_{2d} \rangle = \frac{[\beta_d S_d - (\mu_d + d_d)][\Lambda_d - S_d(\beta_d I_d + \mu_d)]}{\beta_d S_d}$$

$$+ \frac{[(\mu_d + d_d + c)(\beta_d I_d + \mu_d) - \Lambda_d \beta_d][\beta_d S_d - (\mu_d + d_d + c)]}{\beta_d(\mu_d + d_d + c)}$$

$$< \frac{(\mu_d + d_d + c)[\beta_d S_d - (\mu_d + d_d)][\Lambda_d - S_d(\beta_d I_T + \mu_d)]}{\beta_d S_d(\mu_d + d_d + c)}$$

$$+ \frac{S_d[(\mu_d + d_d + c)(\beta_d I_T + \mu_d) - \Lambda_d \beta_d][\beta_d S_d - (\mu_d + d_d)]}{\beta_d S_d(\mu_d + d_d + c)}$$

where $I_d = I_T$, $(\mu_d + d_d + c)(\beta_d I_T + \mu_d) - \Lambda_d \beta_d > 0$ and

$$\times [(\mu_d + d_d + c)(\beta_d I_T + \mu_d) - \Lambda_d \beta_d][\beta_d S_d - (\mu_d + d_d + c)]$$

$$< [(\mu_d + d_d + c)(\beta_d I_T + \mu_d) - \Lambda_d \beta_d][\beta_d S_d - (\mu_d + d_d)]$$

$$= \frac{\Lambda_d[\beta_d S_d - (\mu_d + d_d)][(\mu_d + d_d + c) - \beta_d S_d]}{\beta_d S_d(\mu_d + d_d + c)}$$

$$\leq 0 \quad \forall S_d \leq \frac{\mu_d + d_d}{\beta_d}$$

where $\beta_d S_d - (\mu_d + d_d) \leq 0$, $(\mu_d + d_d + c) - \beta_d S_d > 0$ $\forall S_d \leq \frac{\mu_d + d_d}{\beta_d}$ and $\langle \nabla V, f_{2d} \rangle = 0$ when $S_d = \frac{\mu_d + d_d}{\beta_d}$.
Hence $\sup_{0 \leq \alpha \leq 1} \langle \nabla V, \alpha f_{1d} + (1 - \alpha) f_{2d} \rangle = 0$.

(c) We claim that, under the condition of $(S_d, I_d) \in \left\{ (S_d, I_d) \in M_d; S_d > \frac{\mu_d + d_d}{\beta_d} \right\}$, we have $\sup_{0 \leq \alpha \leq 1} \langle \nabla V, \alpha f_{1d} + (1 - \alpha) f_{2d} \rangle < 0$.

For $I_d = I_T$ and $S_d > \frac{\mu_d + d_d}{\beta_d}$, we obtain $V_1(S_d, I_T) > 0$. Next,

$$\langle \nabla V, f_{1d} \rangle = \langle \nabla V, f_{2d} \rangle$$

$$= \frac{[\beta_d S_d - (\mu_d + d_d)][\Lambda_d - S_d(\beta_d I_T + \mu_d)]}{\beta_d S_d} \quad \text{where } I_d = I_T$$

$$< \frac{[\beta_d S_d - (\mu_d + d_d)]\left(\Lambda_d - \frac{\Lambda_d \beta_d S_d}{\mu_d + d_d}\right)}{\beta_d S_d} \quad \text{where } -(\beta_d I_T + \mu_d) < -\frac{\Lambda_d \beta_d}{\mu_d + d_d}$$

$$= \frac{-\Lambda_d[\beta_d S_d - (\mu_d + d_d)]^2}{\beta_d S_d(\mu_d + d_d)}$$

$$< 0 \quad \forall S_d > \frac{\mu_d + d_d}{\beta_d}.$$

Hence, $\sup_{0 \leq \alpha \leq 1} \langle \nabla V, \alpha f_{1d} + (1 - \alpha) f_{2d} \rangle < 0$.

(d) We want to show that, whenever the condition $(S_d, I_d) \in G_{2d} := \{(S_d, I_d) \in \mathbb{R}_+^2; I_d > I_T\}$ is satisfied, we obtain $\langle \nabla V, f_{2d} \rangle < 0$.

For $I_d > I_T$, it follows that $V_1(S_d, I_d) > 0$. Next,

$$\langle \nabla V, f_{2d} \rangle = \langle \nabla V_1, f_{2d} \rangle$$

$$= \frac{-\Lambda_d[\beta_d S_d - (\mu_d + d_d)]^2 - c S_d[(\mu_d + d_d)(\mu_d + \beta_d I_d) - \Lambda_d \beta_d]}{\beta_d S_d(\mu_d + d_d)}$$

$$< \frac{-\Lambda_d[\beta_d S_d - (\mu_d + d_d)]^2 - c S_d[(\mu_d + d_d)(\mu_d + \beta_d I_T) - \Lambda_d \beta_d]}{\beta_d S_d(\mu_d + d_d)}$$

$$< 0 \quad \forall (S_d, I_d) \in G_{2d}$$

since $-c S_d[(\mu_d + d_d)(\mu_d + \beta_d I_d) - \Lambda_d \beta_d] < -c S_d[(\mu_d + d_d)(\mu_d + \beta_d I_T) - \Lambda_d \beta_d]$ and $(\mu_d + d_d)(\mu_d + \beta_d I_T) - \Lambda_d \beta_d > 0$.
We obtain $\dot{V}^* \equiv \max_{\eta \in f_{id}(S_d, I_d)} \langle \nabla V, \eta \rangle \leq 0$ $\forall (S_d, I_d) \in \mathbb{R}_+^2$ and with equality only if $S_d = \frac{\mu_d + d_d}{\beta_d}$ where $i = 1, 2$ and

$$f_{id}(S_d, I_d) := \begin{cases} f_{1d}; & (S_d, I_d) \in G_{1d} \\ \alpha f_{1d} + (1 - \alpha) f_{2d}; & (S_d, I_d) \in M_d \text{ where } \alpha \in [0, 1] \\ f_{2d}; & (S_d, I_d) \in G_{2d}. \end{cases}$$

Thus $V(S_d, I_d)$ is a Lyapunov function on D_d and, by Lemma 2.1, D_d is compact. Let $\Sigma_{1d} := \{(S_d, I_d) \in \mathbb{R}_+^2; \dot{V}^* = 0\} = G_{1d} \bigcup \left(\frac{\mu_d + d_d}{\beta_d}, I_T \right)$. So the largest positively invariant subset of $\overline{\Sigma}_{1d}$ is $\{E_{11d}^R\}$. Hence, by LaSalle's Invariance Principle and
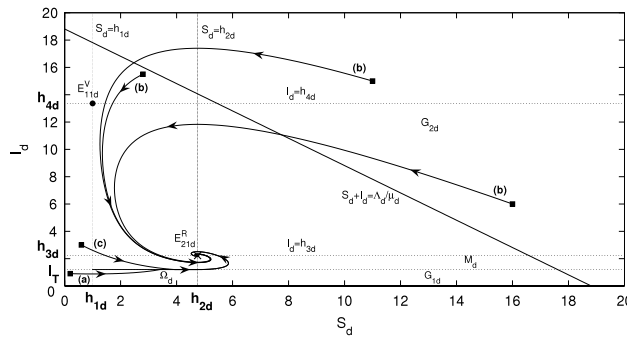
Fig. 7. All trajectories will remain in region $D_d = \left\{ (S_d, I_d) \in \mathbb{R}_+^2 ; I_d + S_d \leq \frac{\Lambda_d}{\mu_d} \right\}$ and converge to $E_{21d}^R \in G_{2d}$ as $t \to \infty$ if $I_T < h_{3d}$ is satisfied.

Corollary C.2 (see Appendix C), every solution of (2.1) with initial conditions in $\mathbb{R}_+^2$ will approach E_{11d}^R as $t \to \infty$ if $I_T > h_{4d}$. Therefore E_{11d}^R is globally asymptotically stable if $I_T > h_{4d}$. ∎

Fig. 4 describes the possible trajectories for Case 2 with $I_T = 65$. The solutions for Case 2 with initial points in G_{1d} will move to E_{11d}^R in G_{1d}, whereas trajectories with initial conditions in G_{2d} will either converge to E_{11d}^R after crossing M_d or hit and slide to the left of Ω_d before moving towards E_{11d}^R.

By applying the same reasoning as in Case 1, we choose $\mu_d = 0.3$ and $I_T = 15$ in Fig. 5. The possible trajectories, which are illustrated in Fig. 5, are as follows:

(a) a trajectory with initial point located in G_{1d} within D_d will converge directly to E_{11d}^R.
(b) a trajectory with initial point located either in G_{1d} or G_{2d} and outside the attracting region D_d will hit and slide to the left of Ω_d before moving towards E_{11d}^R in region G_{1d}.
(c) a trajectory that begins in region G_{1d} outside the attracting region D_d will cross the discontinuous surface M_d. Then it will hit and slide to the left of Ω_d before converging to E_{11d}^R in G_{1d}.

2.4.3. Case 3: E_{21d} is a real equilibrium, whereas E_{11d} is a virtual equilibrium if $I_T < h_{3d}$

Let us denote E_{21d}^R as a real equilibrium and E_{11d}^V as a virtual equilibrium. Both of these equilibria are located in region G_{2d}, and there is no equilibrium lying in region G_{1d}. Further, we claim that E_{21d}^R achieves global asymptotic stability if $I_T < h_{3d}$. In order to show the global behavior of E_{21d}^R, we consider the Lyapunov function $V_2(S_d, I_d)$ (2.13) for model (2.1) and the construction of Theorem 2.8.

Theorem 2.8. *The function $V_2(S_d, I_d)$ (2.13) is a Lyapunov function on $\mathbb{R}_+^2$ for (2.1) and $\{E_{21d}^R\}$ is globally asymptotically stable if $I_T < h_{3d}$.*

The proof of Theorem 2.8 is similar to that of Theorem 2.7.

We depict Theorem 2.8 numerically in Fig. 6. It is clearly shown that every solution of Case 3 will approach E_{21d}^R as $t \to \infty$ with arbitrary initial conditions in $\mathbb{R}_+^2$. Trajectories, which are depicted in Fig. 6, are

(a) a trajectory that starts in region G_{1d} or G_{2d} will hit and slide to the right of Ω_d before moving towards E_{21d}^R.
(b) a trajectory with initial condition in G_{2d} will approach E_{21d}^R as $t \to \infty$.
(c) a trajectory with initial point in G_{1d} may pass through M_d and then proceed towards E_{21d}^R in region G_{2d}.

We increase the parameter μ_d to 0.3 in Fig. 7 to show that the numerical solutions of Case 3 remain in region D_d and converge to E_{21d}^R as $t \to \infty$. In this simulation, we select $I_T = 1.2$. From Fig. 7, we can see that

(a) a trajectory with initial point located in G_{1d} within D_d will hit and slide to the right of $\Omega_d \subset M_d$ before moving towards E_{21d}^R in region G_{2d}.
(b) a trajectory with initial point located in G_{2d} and either within or outside of the attraction region D_d will approach to E_{21d}^R directly.
(c) a trajectory that begins from G_{2d} might hit $\Omega_d \subset M_d$ and slide to the right before moving towards E_{21d}^R.

For Fig. 8, we set $\Lambda_d = 100$, $\mu_d = 0.3$, $\beta_d = 0.01$, $d_d = 0.05$, $c = 0.5$ and $I_T = 50$. We observe that all trajectories with arbitrary initial conditions converge to E_{21d}^R, which agrees with the theoretical result shown in Theorem 2.8.

In conclusion, the solutions of model (2.1) will converge to either one of the two endemic equilibria (i.e., either E_{11d}^R in G_{1d} or E_{21d}^R in G_{2d}) or the sliding equilibrium E_d on sliding domain $\Omega_d \subset M_d$ if the requirement of (2.8) is met. We do not have to apply any control methods whenever $h_{3d} < I_T < h_{4d}$ (Case 1) or $I_T > h_{4d}$ (Case 2) is satisfied. This is due to the number of infected birds, which always remain below the given threshold level I_T since we have proclaimed that the infection is tolerable. Therefore, in this particular case, the trajectory of model (2.1) either converges to E_{11d}^R in G_{1d} or stabilizes at E_d
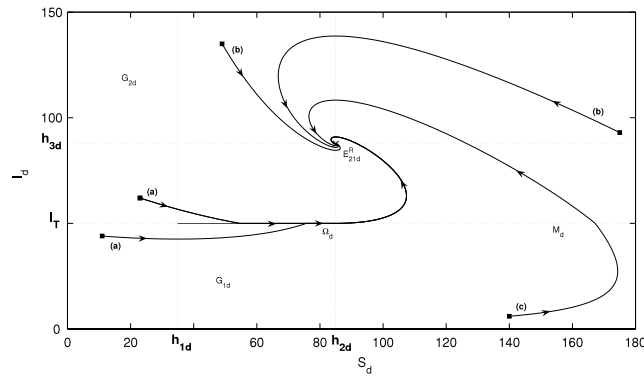
Fig. 8. $E_{21d}^R \in G_{2d}$ achieves global asymptotic stability whenever $I_T < h_{3d}$.

on $\Omega_d \subset M_d$. However, the solution of (2.1) converges to E_{21d}^R in G_{2d} if $I_T < h_{3d}$ (Case 3). For this case, the application of control methods will be triggered as the number of infected birds reaches the critical level (i.e., greater than the tolerance threshold level I_T), beyond which we proclaim that an outbreak will occur. In order to inhibit the occurrence of an outbreak or stabilize the infection at a satisfactory level, by virtue of Theorem 2.6, we need a proper combination of control intensity and tolerance level. Hence, in order to combat an outbreak effectively, we require a well-defined threshold policy.

3. The SIIR model with quarantine as a control measure

When six people were reported dead and 18 people infected by H5N1 in Hong Kong in 1997, it changed the general belief that avian influenza viruses were believed to be non-infectious to humans. Most avian influenza viruses do not spread to humans; however, H5N1, H7N2, H7N3, H7N7 and H7N9 are known to cause severe infections in humans [26,38,39]. Avian influenza viruses transmit easily to humans through direct contact with dead or infected birds. However, there are some reported cases that humans might be infected by the lethal virus indirectly via contaminated water, food that has been stained by the virus or other objects contaminated with infected birds' feces [26,40].

There are many types of control methods that have been employed to reduce the infection rate of avian influenza, such as practicing personal protection, isolation, prescription of antiviral drugs and vaccination [18,14,15]. So in this section, we would like to consider a Filippov SIIR avian influenza model incorporating quarantine as a control measure. This model consists of susceptibles (S), humans infected with avian strain (I_a), humans infected with mutant strain (I_m) and humans who have recovered from avian and mutant strains (R). Here, we assume that when the total number of infected humans, $I_a + I_m$, is greater than some threshold level I_c, infected humans with either avian or mutant strain will be isolated from susceptibles. In other words, quarantine will be implemented in order to control the spread of the disease and the quarantined individuals will not return to the susceptible population; that is, the immunity was permanent. However, if the total number of infected humans is below the tolerance threshold I_c, then quarantine is not required. The SIIR model equations can be expressed as:

$$
\begin{aligned}
S'(t) &= \Lambda - \beta_a(1 - qu)SI_a - \beta_m(1 - qu)SI_m - \mu S \\
I_a'(t) &= \beta_a(1 - qu)SI_a - (\mu + d + \gamma + \epsilon)I_a \\
I_m'(t) &= \beta_m(1 - qu)SI_m + \epsilon I_a - (\mu + d + \gamma)I_m \\
R'(t) &= \gamma(I_a + I_m) - \mu R
\end{aligned}
\tag{3.1}
$$

with

$$
u = \begin{cases} 0 & \text{for } I_a + I_m < I_c \Leftrightarrow \sigma(I_a, I_m) = I_a + I_m - I_c < 0 \\ 1 & \text{for } I_a + I_m > I_c \Leftrightarrow \sigma(I_a, I_m) = I_a + I_m - I_c > 0, \end{cases}
\tag{3.2}
$$

where q is the quarantine rate and $I_c > 0$ is the critical threshold of the total number of infected humans. Table 2 shows the descriptions of the associated parameters in model (3.1) and sample values.

Since R decouples from the remaining equations in model (3.1), we consider only the first three equations of model (3.1) with (3.2). It should be noted that R always preserves local stability; i.e., the associated eigenvalue is $\lambda = -\mu < 0$ where $\mu > 0$. We further assume that $\beta_a > \beta_m$ [37]. Furthermore, we define

$$
\begin{aligned}
G_1 &:= \{(S, I_a, I_m) \in \mathbb{R}_+^3; I_a + I_m < I_c\} \\
G_2 &:= \{(S, I_a, I_m) \in \mathbb{R}_+^3; I_a + I_m > I_c\} \\
M &:= \{(S, I_a, I_m) \in \mathbb{R}_+^3; I_a + I_m = I_c\}.
\end{aligned}
$$

Table 2
Descriptions of the associated parameters in SIIR model (3.1) and sample values.

Parameter	Description	Sample value	Units	Reference
Λ	Human recruitment rate	$\frac{1000}{365}$	Individuals per day	[36]
μ	Natural mortality rate of humans	$\frac{1}{65 \times 365}$	per day	[36]
β_a	Transmission rate of human-to-human with avian strain	0.4	per individual per day	[37]
β_m	Transmission rate of human-to-human with mutant strain	$0.3 \times \beta_a$	per individual per day	[37]
d	Additional disease death rate of humans due to avian influenza	0.15	per day	[36]
γ	Recovery rate of humans with avian influenza	0.2669	per day	[41]
ϵ	Mutation rate	0.01	per day	[37]
q	Quarantine rate	0.6	Assumed	

The manifold M is a discontinuous surface and it divides $\mathbb{R}^3_+$ into two regions, G_1 and G_2. We denote the normal vector that is perpendicular to M as $n = (0, 1, 1)^T$ and all the right-hand sides of (3.1) in region G_i by f_i for $i = 1, 2$. The dynamical systems in regions G_1 and G_2 are thus represented by

$$f_1 = f_1(S, I_a, I_m) = \begin{pmatrix} \Lambda - \beta_a SI_a - \beta_m SI_m - \mu S \\ \beta_a SI_a - (\mu + d + \gamma + \epsilon)I_a \\ \beta_m SI_m + \epsilon I_a - (\mu + d + \gamma)I_m \end{pmatrix}$$

$$f_2 = f_2(S, I_a, I_m) = \begin{pmatrix} \Lambda - (1 - q)\beta_a SI_a - (1 - q)\beta_m SI_m - \mu S \\ (1 - q)\beta_a SI_a - (\mu + d + \gamma + \epsilon)I_a \\ (1 - q)\beta_m SI_m + \epsilon I_a - (\mu + d + \gamma)I_m \end{pmatrix}. \tag{3.3}$$

Lemma 3.1. *The set* $D = \left\{ (S, I_a, I_m, R) \in \mathbb{R}^4_+; N = S + I_a + I_m + R \le \frac{\Lambda}{\mu} \right\}$ *is a positively invariant and attracting region for* (3.1) *with any initial conditions in* $\mathbb{R}^4_+$.

We can use a similar method as shown in Lemma 2.1 to prove Lemma 3.1; hence we omit the proof of this lemma.

Since D is a positively invariant and attracting region for model (3.1), the solution of (3.1) exists in $D \; \forall t > 0$ and model (3.1) is mathematically and epidemiologically well-posed in D [30]. Thus it is sufficient to consider the dynamics of this model in D.

3.1. Analysis in region G_1

The dynamical systems in region G_1 can be described by the following nonlinear ordinary differential equations.

$$\begin{pmatrix} S'(t) \\ I'_a(t) \\ I'_m(t) \end{pmatrix} = \begin{pmatrix} \Lambda - \beta_a SI_a - \beta_m SI_m - \mu S \\ \beta_a SI_a - (\mu + d + \gamma + \epsilon)I_a \\ \beta_m SI_m + \epsilon I_a - (\mu + d + \gamma)I_m \end{pmatrix} := f_1. \tag{3.4}$$

There are two equilibria in G_1, the DFE $E_{10} = (S, I_a, I_m) = \left(\frac{\Lambda}{\mu}, 0, 0 \right)$ and a unique positive EE

$$E_{11} = (E_{11}S, E_{11}I_a, E_{11}I_m)$$

where

$$E_{11}S = \frac{\mu + d + \gamma + \epsilon}{\beta_a}$$

$$E_{11}I_m = \frac{\epsilon \left[\Lambda \beta_a - \mu(\mu + d + \gamma + \epsilon) \right]}{(\beta_a - \beta_m)(\mu + d + \gamma)(\mu + d + \gamma + \epsilon)}$$

$$E_{11}I_a = \frac{\left[\Lambda \beta_a - \mu(\mu + d + \gamma + \epsilon) \right] \left[(\mu + d + \gamma)(\beta_a - \beta_m) - \epsilon \beta_m \right]}{\beta_a(\beta_a - \beta_m)(\mu + d + \gamma)(\mu + d + \gamma + \epsilon)}$$

$$= \frac{\left[(\mu + d + \gamma)(\beta_a - \beta_m) - \epsilon \beta_m \right] E_{11}I_m}{\epsilon \beta_a}.$$

In $G_1 := \left\{ (S, I_a, I_m) \in \mathbb{R}^3_+; I_m < -I_a + I_c \right\}$, we have $E_{11} \in \mathbb{R}^3_+$, and this implies that

$$E_{11}S = \frac{\mu + d + \gamma + \epsilon}{\beta_a} > 0 \tag{3.5}$$

$$E_{11}I_m = \frac{\epsilon \left[\Lambda \beta_a - \mu(\mu + d + \gamma + \epsilon) \right]}{(\beta_a - \beta_m)(\mu + d + \gamma)(\mu + d + \gamma + \epsilon)} > 0,$$

which implies $\Lambda\beta_a - \mu(\mu + d + \gamma + \epsilon) > 0$ since $\beta_a > \beta_m$ and

$$E_{11}I_a = \frac{[(\mu + d + \gamma)(\beta_a - \beta_m) - \epsilon\beta_m]E_{11}I_m}{\epsilon\beta_a} > 0, \tag{3.6}$$

which implies $(\mu + d + \gamma)\beta_a - (\mu + d + \gamma + \epsilon)\beta_m > 0$ since $\beta_a > \beta_m$ and $E_{11}I_m > 0$.

The transmission matrix F_1 and transition matrix V_1 of model (3.4) are defined as

$$F_1 = \begin{pmatrix} \beta_a S & 0 \\ 0 & \beta_m S \end{pmatrix} \quad \text{and} \quad V_1 = \begin{pmatrix} \mu + d + \gamma + \epsilon & 0 \\ -\epsilon & \mu + d + \gamma \end{pmatrix}, \quad \text{respectively.}$$

At the DFE, we have

$$F_1 V_1^{-1} = \begin{pmatrix} \dfrac{\Lambda\beta_a}{\mu(\mu + d + \gamma + \epsilon)} & 0 \\ \dfrac{\Lambda\beta_m\epsilon}{\mu(\mu + d + \gamma)(\mu + d + \gamma + \epsilon)} & \dfrac{\Lambda\beta_m}{\mu(\mu + d + \gamma)} \end{pmatrix}$$

and the basic reproduction number (see [31,32] for more details) of G_1 is given as follows:

$$R_1 := \max\left\{\frac{\Lambda\beta_a}{\mu(\mu + d + \gamma + \epsilon)}, \frac{\Lambda\beta_m}{\mu(\mu + d + \gamma)}\right\} = \max\{R_{1a}, R_{1m}\}$$

where $R_{1a} = \frac{\Lambda\beta_a}{\mu(\mu+d+\gamma+\epsilon)}$ and $R_{1m} = \frac{\Lambda\beta_m}{\mu(\mu+d+\gamma)}$.

The Jacobian matrix of model (3.4) is

$$J_1(S, I_a, I_m) = \begin{pmatrix} -\beta_a I_a - \beta_m I_m - \mu & -\beta_a S & -\beta_m S \\ \beta_a I_a & \beta_a S - (\mu + d + \gamma + \epsilon) & 0 \\ \beta_m I_m & \epsilon & \beta_m S - (\mu + d + \gamma) \end{pmatrix}.$$

Further, the local asymptotic stability of E_{10} and E_{11} is shown in the following theorems.

Theorem 3.2. *For model* (3.4), *the DFE E_{10} is locally asymptotically stable if $R_1 < 1$.*

As in the proof of Theorem 2.2, we can show that all eigenvalues of (3.4) at E_{10} are negative if $R_1 < 1$. Hence E_{10} achieves local asymptotic stability whenever $R_1 < 1$.

Theorem 3.3. *For model* (3.4), *the endemic equilibrium E_{11} is locally asymptotically stable if $R_1 > 1$, $a_1, a_2, a_3 > 0$ and $a_1 a_2 > a_3$, where*
$a_1 = \frac{\Lambda\beta_a}{\mu+d+\gamma+\epsilon} + \frac{(\mu+d+\gamma)\beta_a-(\mu+d+\gamma+\epsilon)\beta_m}{\beta_a}$,
$a_2 = \frac{[\Lambda\beta_a-\mu(\mu+d+\gamma+\epsilon)][\beta_a(\mu+d+\gamma)-\epsilon\beta_m]}{\beta_a(\mu+d+\gamma)} + \frac{\Lambda[\beta_a(\mu+d+\gamma)-\beta_m(\mu+d+\gamma+\epsilon)]}{\mu+d+\gamma+\epsilon}$ *and*
$a_3 = \frac{[\Lambda\beta_a-\mu(\mu+d+\gamma+\epsilon)][(\mu+d+\gamma)\beta_a-(\mu+d+\gamma+\epsilon)\beta_m]}{\beta_a}$.

Proof. At E_{11}, the Jacobian matrix is

$$J_1(E_{11}) = \begin{pmatrix} A_{11} & A_{12} & A_{13} \\ A_{21} & A_{22} & A_{23} \\ A_{31} & A_{32} & A_{33} \end{pmatrix}$$

where $A_{11} = -\frac{\Lambda\beta_a}{\mu+d+\gamma+\epsilon}$, $A_{12} = -(\mu + d + \gamma + \epsilon)$, $A_{13} = -\frac{\beta_m(\mu+d+\gamma+\epsilon)}{\beta_a}$, $A_{21} = \frac{[\Lambda\beta_a-\mu(\mu+d+\gamma+\epsilon)][(\mu+d+\gamma)\beta_a-(\mu+d+\gamma+\epsilon)\beta_m]}{(\beta_a-\beta_m)(\mu+d+\gamma)(\mu+d+\gamma+\epsilon)}$, $A_{22} = A_{23} = 0$, $A_{31} = \frac{\epsilon\beta_m[\Lambda\beta_a-\mu(\mu+d+\gamma+\epsilon)]}{(\beta_a-\beta_m)(\mu+d+\gamma)(\mu+d+\gamma+\epsilon)}$, $A_{32} = \epsilon$ and $A_{33} = \frac{(\mu+d+\gamma+\epsilon)\beta_m-(\mu+d+\gamma)\beta_a}{\beta_a}$.

By solving the characteristic equation $|J_1(E_{11}) - \lambda I| = 0$, we obtain

$$\lambda^3 + \left[\frac{\Lambda\beta_a}{\mu + d + \gamma + \epsilon} + \frac{(\mu + d + \gamma)\beta_a - (\mu + d + \gamma + \epsilon)\beta_m}{\beta_a}\right]\lambda^2$$

$$+ \left\{\frac{\left[\Lambda\beta_a - \mu(\mu + d + \gamma + \epsilon)\right]\left[\beta_a(\mu + d + \gamma) - \epsilon\beta_m\right]}{\beta_a(\mu + d + \gamma)} + \frac{\Lambda\left[\beta_a(\mu + d + \gamma) - \beta_m(\mu + d + \gamma + \epsilon)\right]}{\mu + d + \gamma + \epsilon}\right\}\lambda$$

$$+ \frac{\left[\Lambda\beta_a - \mu(\mu + d + \gamma + \epsilon)\right]\left[(\mu + d + \gamma)\beta_a - (\mu + d + \gamma + \epsilon)\beta_m\right]}{\beta_a} = 0. \tag{3.7}$$

If $R_1 > 1 \implies R_{1a} > 1 \implies \Lambda\beta_a - \mu(\mu + d + \gamma + \epsilon) > 0$ and $\beta_a(\mu + d + \gamma) - \beta_m(\mu + d + \gamma + \epsilon) > 0$ from (3.6) $\implies \beta_a(\mu + d + \gamma) - \epsilon\beta_m > 0$, then we obtain $a_1, a_2, a_3 > 0$. Moreover, if we also have $a_1 a_2 > a_3$, then, by the Routh–Hurwitz Criterion [42], all roots of (3.7) are negative or have negative real parts. Hence E_{11} is locally asymptotically stable if $R_1 > 1$ and $a_1 a_2 > a_3$. ∎

3.2. Analysis in region G_2

The dynamics in region G_2 can be represented by nonlinear ordinary differential equations as follows:

$$\begin{pmatrix} S'(t) \\ I_a'(t) \\ I_m'(t) \end{pmatrix} = \begin{pmatrix} \Lambda - \beta_a(1-q)SI_a - \beta_m(1-q)SI_m - \mu S \\ \beta_a(1-q)SI_a - (\mu+d+\gamma+\epsilon)I_a \\ \beta_m(1-q)SI_m + \epsilon I_a - (\mu+d+\gamma)I_m \end{pmatrix} := f_2. \tag{3.8}$$

In G_2, we have two equilibria: the DFE, $E_{20} = (S, I_a, I_m) = \left(\frac{\Lambda}{\mu}, 0, 0\right)$, and a unique positive EE,

$$E_{21} = (E_{21}S, E_{21}I_a, E_{21}I_m),$$

where

$$E_{21}S = \frac{\mu+d+\gamma+\epsilon}{\beta_a(1-q)}$$

$$E_{21}I_m = \frac{\epsilon[\Lambda\beta_a(1-q) - \mu(\mu+d+\gamma+\epsilon)]}{(1-q)(\beta_a-\beta_m)(\mu+d+\gamma)(\mu+d+\gamma+\epsilon)}$$

$$E_{21}I_a = \frac{[\Lambda\beta_a(1-q) - \mu(\mu+d+\gamma+\epsilon)][(\mu+d+\gamma)\beta_a - (\mu+d+\gamma+\epsilon)\beta_m]}{\beta_a(1-q)(\beta_a-\beta_m)(\mu+d+\gamma)(\mu+d+\gamma+\epsilon)}$$

$$= \frac{[(\mu+d+\gamma)\beta_a - (\mu+d+\gamma+\epsilon)\beta_m]E_{21}I_m}{\epsilon\beta_a}.$$

Furthermore, we have $E_{21} \in \mathbb{R}^3_+$, and this implies that

$$E_{21}S = \frac{\mu+d+\gamma+\epsilon}{\beta_a(1-q)} > 0$$

$$E_{21}I_m = \frac{\epsilon[\Lambda\beta_a(1-q) - \mu(\mu+d+\gamma+\epsilon)]}{(1-q)(\beta_a-\beta_m)(\mu+d+\gamma)(\mu+d+\gamma+\epsilon)} > 0,$$

which implies $\Lambda\beta_a(1-q) - \mu(\mu+d+\gamma+\epsilon) > 0$, where $0 < 1-q < 1$ and $\beta_a > \beta_m \Longrightarrow \beta_a - \beta_m > 0$ and

$$E_{21}I_a = \frac{[(\mu+d+\gamma)\beta_a - (\mu+d+\gamma+\epsilon)\beta_m]E_{21}I_m}{\epsilon\beta_a} > 0,$$

which implies $(\mu+d+\gamma)\beta_a - (\mu+d+\gamma+\epsilon)\beta_m > 0$ with $E_{21}I_m > 0$.

The transmission matrix, F_2, and transition matrix, V_2, of model (3.8) are

$$F_2 = \begin{pmatrix} \beta_a(1-q)S & 0 \\ 0 & \beta_m(1-q)S \end{pmatrix} \quad \text{and} \quad V_2 = \begin{pmatrix} \mu+d+\gamma+\epsilon & 0 \\ -\epsilon & \mu+d+\gamma \end{pmatrix}, \quad \text{respectively.}$$

At the DFE E_{20}, we have

$$F_2 V_2^{-1} = \begin{pmatrix} \dfrac{\Lambda\beta_a(1-q)}{\mu(\mu+d+\gamma+\epsilon)} & 0 \\ \dfrac{\epsilon\Lambda\beta_m(1-q)}{\mu(\mu+d+\gamma)(\mu+d+\gamma+\epsilon)} & \dfrac{\Lambda\beta_m(1-q)}{\mu(\mu+d+\gamma)} \end{pmatrix}$$

and the basic reproduction number (see [31,32] for further details) of G_2 is

$$R_2 := \max\left\{\frac{\Lambda\beta_a(1-q)}{\mu(\mu+d+\gamma+\epsilon)}, \frac{\Lambda\beta_m(1-q)}{\mu(\mu+d+\gamma)}\right\} = \max\{R_{2a}, R_{2m}\}$$

where $R_{2a} = \frac{\Lambda\beta_a(1-q)}{\mu(\mu+d+\gamma+\epsilon)}$ and $R_{2m} = \frac{\Lambda\beta_m(1-q)}{\mu(\mu+d+\gamma)}$.

In addition, the Jacobian matrix of model (3.8) is

$$J_2(S, I_a, I_m) = \begin{pmatrix} B_{11} & B_{12} & B_{13} \\ B_{21} & B_{22} & B_{23} \\ B_{31} & B_{32} & B_{33} \end{pmatrix}$$

where $B_{11} = -\beta_a(1-q)I_a - \beta_m(1-q)I_m - \mu$, $B_{12} = -\beta_a(1-q)S$, $B_{13} = -\beta_m(1-q)S$, $B_{21} = \beta_a(1-q)I_a$, $B_{22} = \beta_a(1-q)S - (\mu+d+\gamma+\epsilon)$, $B_{23} = 0$, $B_{31} = \beta_m(1-q)I_m$, $B_{32} = \epsilon$ and $B_{33} = \beta_m(1-q)S - (\mu+d+\gamma)$.

Furthermore, the local asymptotic stability of E_{21} and E_{21} is shown in the following theorems.

Theorem 3.4. *For model* (3.8)*, the DFE E_{20} is locally asymptotically stable if $R_2 < 1$.*

We use a similar method as shown in Theorem 3.2 to prove Theorem 3.4; i.e., to show that all eigenvalues of model (3.8) at E_{20} are negative if $R_2 < 1$.

Theorem 3.5. *For model* (3.8), *the endemic equilibrium* E_{21} *is locally asymptotically stable if* $R_2 > 1$, b_1, b_2, $b_3 > 0$ *and* $b_1 b_2 > b_3$, *where*

$$b_1 = \frac{\Lambda \beta_a (1-q)}{\mu + d + \gamma + \epsilon} + \frac{(\mu + d + \gamma)\beta_a - (\mu + d + \gamma + \epsilon)\beta_m}{\beta_a}$$

$$b_2 = \frac{[\Lambda \beta_a (1-q) - \mu(\mu + d + \gamma + \epsilon)][\beta_a(\mu + d + \gamma) - \epsilon \beta_m]}{\beta_a(\mu + d + \gamma)}$$
$$+ \frac{\Lambda(1-q)[\beta_a(\mu + d + \gamma) - \beta_m(\mu + d + \gamma + \epsilon)]}{\mu + d + \gamma + \epsilon}$$

$$b_3 = \frac{[\Lambda \beta_a (1-q) - \mu(\mu + d + \gamma + \epsilon)][(\mu + d + \gamma)\beta_a - (\mu + d + \gamma + \epsilon)\beta_m]}{\beta_a}.$$

Similar methods as Theorem 3.3 can be used to demonstrate the proof of Theorem 3.5; thus we omit the proof of this theorem.

3.3. Existence of sliding mode and its dynamical systems

We need to compute

$$\langle n, f_1 \rangle = \left\langle \begin{pmatrix} 0 \\ 1 \\ 1 \end{pmatrix}, \begin{pmatrix} \Lambda - \beta_a S I_a - \beta_m S I_m - \mu S \\ \beta_a S I_a - (\mu + d + \gamma + \epsilon) I_a \\ \beta_m S I_m + \epsilon I_a - (\mu + d + \gamma) I_m \end{pmatrix} \right\rangle$$
$$= \beta_a S I_a + \beta_m S I_m - (\mu + d + \gamma)(I_a + I_m)$$
$$= \beta_a S I_a + \beta_m S I_m - (\mu + d + \gamma) I_c \qquad (3.9)$$

where, on M, we have $I_m = -I_a + I_c$ and

$$\langle n, f_2 \rangle = \left\langle \begin{pmatrix} 0 \\ 1 \\ 1 \end{pmatrix}, \begin{pmatrix} \Lambda - \beta_a(1-q)S I_a - \beta_m(1-q)S I_m - \mu S \\ \beta_a(1-q)S I_a - (\mu + d + \gamma + \epsilon) I_a \\ \beta_m(1-q)S I_m + \epsilon I_a - (\mu + d + \gamma) I_m \end{pmatrix} \right\rangle$$
$$= \beta_a(1-q)S I_a + \beta_m(1-q)S I_m - (\mu + d + \gamma)(I_a + I_m)$$
$$= \beta_a(1-q)S I_a + \beta_m(1-q)S(I_c - I_a) - (\mu + d + \gamma) I_c$$
$$= (\beta_a - \beta_m)(1-q)S I_a + \beta_m(1-q)S I_c - (\mu + d + \gamma) I_c. \qquad (3.10)$$

A sliding mode exists if $\langle n, f_1 \rangle > 0$ and $\langle n, f_2 \rangle < 0$. Thus

$$\langle n, f_1 \rangle > 0 \quad \text{if } S > h_1(I_a) := \frac{(\mu + d + \gamma) I_c}{(\beta_a - \beta_m) I_a + \beta_m I_c}$$

$$\langle n, f_2 \rangle < 0 \quad \text{if } S < h_2(I_a) := \frac{(\mu + d + \gamma) I_c}{(1-q)[(\beta_a - \beta_m) I_a + \beta_m I_c]}$$

where $0 < 1 - q < 1$. Since $\beta_a > \beta_m$, $0 < 1 - q < 1$ and I_a, $I_c > 0$, then we obtain $h_2(I_a) = \frac{h_1(I_a)}{1-q}$ and $h_1(I_a) < h_2(I_a)$. So the sliding domain $\Omega \subset M$ is defined as

$$\Omega := \{(S, I_a, I_m) \in M; h_1(I_a) < S < h_2(I_a), I_a + I_m = I_c\}.$$

Further, we can find sliding mode equations by using the Utkin equivalent control method [43]. From (3.2), we have $\sigma(I_a, I_m) = I_a + I_m - I_c$. Then,

$$\frac{d\sigma}{dt} = \frac{\partial \sigma}{\partial I_a} \cdot \frac{dI_a}{dt} + \frac{\partial \sigma}{\partial I_m} \cdot \frac{dI_m}{dt}$$
$$= (1 - qu)S(\beta_a I_a + \beta_m I_m) - (\mu + d + \gamma)(I_a + I_m) \quad \text{from (3.1)}.$$

By setting $\frac{d\sigma}{dt} = 0$ and solving for u, we obtain

$$u = \frac{S[(\beta_a - \beta_m)I_a + \beta_m I_c] - (\mu + d + \gamma) I_c}{qS[(\beta_a - \beta_m)I_a + \beta_m I_c]} \qquad (3.11)$$

where, on M, we have $I_m = -I_a + I_c$.

From $\frac{d\sigma}{dt} = 0$, we also have $I_a'(t) + I_m'(t) = 0$. By substituting (3.11) into (3.1), we have

$$S'(t) = \Lambda - (\mu + d + \gamma)I_c - \mu S;$$
$$I_a'(t) = \beta_a I_a \left[\frac{(\mu + d + \gamma)I_c}{(\beta_a - \beta_m)I_a + \beta_m I_c} \right] - (\mu + d + \gamma + \epsilon)I_a. \tag{3.12}$$

So the sliding mode equations on $\Omega \subset M$ are

$$S'(t) = \Lambda - (\mu + d + \gamma)I_c - \mu S$$
$$I_a'(t) = \beta_a I_a \left[\frac{(\mu + d + \gamma)I_c}{(\beta_a - \beta_m)I_a + \beta_m I_c} \right] - (\mu + d + \gamma + \epsilon)I_a \tag{3.13}$$
$$I_m'(t) = -I_a'(t).$$

For model (3.13), there exists a unique positive pseudoequilibrium point, $E_s = (E_s S, E_s I_a, E_s I_m)$, where $E_s S = \frac{\Lambda - (\mu + d + \gamma)I_c}{\mu}$, $E_s I_a = \frac{I_c[\beta_a(\mu + d + \gamma) - \beta_m(\mu + d + \gamma + \epsilon)]}{(\beta_a - \beta_m)(\mu + d + \gamma + \epsilon)}$ and $E_s I_m = \frac{\epsilon \beta_a I_c}{(\beta_a - \beta_m)(\mu + d + \gamma + \epsilon)}$. E_s is in $\Omega \subset M$ if the following constraint is satisfied.

$$h_1(I_a) < E_s S < h_2(I_a) \Leftrightarrow h_1(I_a) < \frac{\Lambda - (\mu + d + \gamma)I_c}{\mu} < h_2(I_a).$$

A reduced dynamical system of (3.13) is defined as in (3.12), and the local asymptotic stability of E_s is shown in the following theorem.

Theorem 3.6. $E_s \in \Omega$ is locally asymptotically stable if $\beta_a(\mu + d + \gamma) - \beta_m(\mu + d + \gamma + \epsilon) > 0$.

A similar approach as in Theorem 2.2 can be employed to demonstrate that all eigenvalues of (3.12) at E_s are negative if $\beta_a(\mu + d + \gamma) - \beta_m(\mu + d + \gamma + \epsilon) > 0$, so we omit the proof of this theorem.

3.4. Local stability of the endemic equilibria

$(S, I_a, I_m) \in \mathbb{R}_+^3$ is divided into three regions, G_1, M and G_2. There exists an equilibrium point in each region, E_{11}, E_s and E_{21} in regions G_1, $\Omega \subset M$ and G_2, respectively. In this section, let us denote the real and virtual equilibria with superscripts R and V, respectively. We will discuss the stability of E_s, E_{11} and E_{21} in the following subsections. Note that, in order to illustrate the theoretical results, some numerical simulations are carried out in this section. All parameters shown in Table 2 are used in the numerical simulations, unless otherwise stated.

3.4.1. Case 1: E_{11} and E_{21} are virtual equilibria
If (3.14) is satisfied, then both E_{11} and E_{21} are virtual equilibria.

$$E_{11}I_a + E_{11}I_m > I_c \quad \text{and} \quad E_{21}I_a + E_{21}I_m < I_c. \tag{3.14}$$

Here E_{11}^V and E_{21}^V are located in regions G_2 and G_1, respectively. In this case, we have $E_s \in \Omega \subset M$, which is locally asymptotically stable. All trajectories will converge to E_s if (3.14) is satisfied.

Theorem 3.7. The pseudoequilibrium E_s cannot coexist with E_{11}^R and E_{21}^R. In addition, $E_s \in \Omega \subset M$ is locally asymptotically stable if it exists.

Proof. Note that $E_s S - h_1(E_s I_a) > (<)0 \implies \Lambda \beta_a - \mu(\mu + d + \gamma + \epsilon) > (<)\beta_a(\mu + d + \gamma)I_c$, $E_s S - h_2(E_s I_a) < (>)0 \implies \Lambda \beta_a(1 - q) - \mu(\mu + d + \gamma + \epsilon) < (>)\beta_a(1 - q)(\mu + d + \gamma)I_c$ where $0 < 1 - q < 1$ and all associated parameters are positive, $E_{11}I_a + E_{11}I_m = \frac{\Lambda \beta_a - \mu(\mu + d + \gamma + \epsilon)}{\beta_a(\mu + d + \gamma)}$ and $E_{21}I_a + E_{21}I_m = \frac{\Lambda \beta_a(1 - q) - \mu(\mu + d + \gamma + \epsilon)}{\beta_a(1 - q)(\mu + d + \gamma)}$. We refer to [44] to prove that the pseudoequilibrium E_s cannot coexist with E_{11}^R and E_{21}^R. So we have to show that (a) if $E_s \in \Omega \subset M$ is a pseudoequilibrium, then E_{11} and E_{21} are virtual equilibria, and (b) if E_s is not a pseudoequilibrium, then E_{11} and E_{21} are real equilibria.

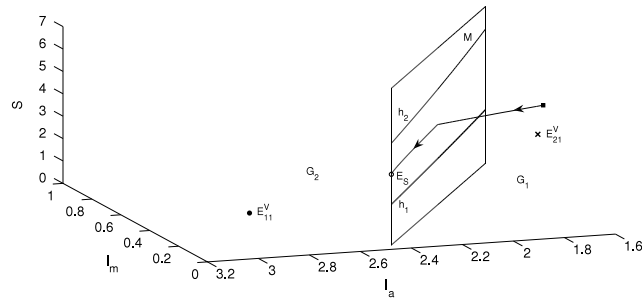(a) If $E_s \in \Omega \subset M$ is a pseudoequilibrium (i.e., $h_1(E_s I_a) < E_s S < h_2(E_s I_a) \implies E_s S - h_1(E_s I_a) > 0$ and $E_s S - h_2(E_s I_a) < 0$), then $E_{11}I_a + E_{11}I_m > I_c$ and $E_{21}I_a + E_{21}I_m < I_c$ indicate that E_{11} and E_{21} are virtual equilibria.

$$E_{11}I_a + E_{11}I_m = \frac{\Lambda \beta_a - \mu(\mu + d + \gamma + \epsilon)}{\beta_a(\mu + d + \gamma)} > \frac{\beta_a(\mu + d + \gamma)I_c}{\beta_a(\mu + d + \gamma)} = I_c$$

where $E_s S - h_1(E_s I_a) > 0 \implies \Lambda \beta_a - \mu(\mu + d + \gamma + \epsilon) > \beta_a(\mu + d + \gamma)I_c$.

$$E_{21}I_a + E_{21}I_m = \frac{\Lambda \beta_a(1 - q) - \mu(\mu + d + \gamma + \epsilon)}{\beta_a(1 - q)(\mu + d + \gamma)} < \frac{\beta_a(1 - q)(\mu + d + \gamma)I_c}{\beta_a(1 - q)(\mu + d + \gamma)} = I_c$$

where $E_s S - h_2(E_s I_a) < 0 \implies \Lambda \beta_a(1 - q) - \mu(\mu + d + \gamma + \epsilon) < \beta_a(1 - q)(\mu + d + \gamma)I_c$. Thus the existence of pseudoequilibrium E_s implies the non-existence of real equilibria E_{11} and E_{21}.

(a) A trajectory with initial point in G_1 will hit and slide to the left on $\Omega \subset M$ before moving towards E_s.

(b) A trajectory which begins in region G_2 will converge to E_s after it hits and slides to the right on $\Omega \subset M$.

Fig. 9. $E_s \in \Omega \subset M$ is locally asymptotically stable if (3.14) is satisfied.

(b) If E_s is not a pseudoequilibrium (i.e., $E_s \notin \Omega \subset M \Longrightarrow E_sS - h_1(E_sI_a) < 0$ and $E_sS - h_2(E_sI_a) > 0$) then $E_{11}I_a + E_{11}I_m < I_c$ and $E_{21}I_a + E_{21}I_m > I_c$ indicate that E_{11} and E_{21} are real equilibria.

$$E_{11}I_a + E_{11}I_m = \frac{\Lambda\beta_a - \mu(\mu + d + \gamma + \epsilon)}{\beta_a(\mu + d + \gamma)} < \frac{\beta_a(\mu + d + \gamma)I_c}{\beta_a(\mu + d + \gamma)} = I_c$$
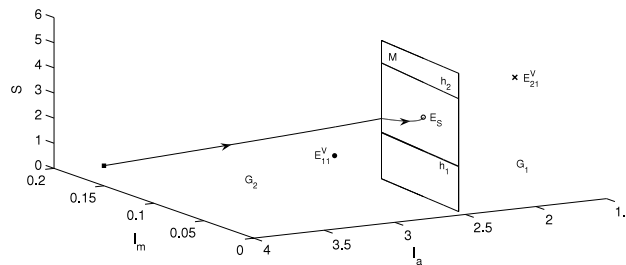
where $E_sS - h_1(E_sI_a) < 0 \Longrightarrow \Lambda\beta_a - \mu(\mu + d + \gamma + \epsilon) < \beta_a(\mu + d + \gamma)I_c$.

$$E_{21}I_a + E_{21}I_m = \frac{\Lambda\beta_a(1 - q) - \mu(\mu + d + \gamma + \epsilon)}{\beta_a(1 - q)(\mu + d + \gamma)} > \frac{\beta_a(1 - q)(\mu + d + \gamma)I_c}{\beta_a(1 - q)(\mu + d + \gamma)} = I_c$$

where $E_sS - h_2(E_sI_a) > 0 \Longrightarrow \Lambda\beta_a(1 - q) - \mu(\mu + d + \gamma + \epsilon) > \beta_a(1 - q)(\mu + d + \gamma)I_c$.

So E_{11} and E_{21} are real equilibria whenever $E_s \notin \Omega \subset M$. Therefore, the pseudoequilibrium E_s cannot coexist with the real equilibria E_{11} and E_{21}.

Next, we would like to discuss the stability of $E_s \in \Omega \subset M$. We have shown that $E_s \in \Omega \subset M$ achieves local asymptotic stability in Theorem 3.6. For any choice of threshold level I_c in between $E_{21}I_a + E_{21}I_m$ and $E_{11}I_a + E_{11}I_m$, the local asymptotic stability of E_s in the sliding domain always holds. Hence, E_s is locally asymptotically stable in the sliding domain $\Omega \subset M$ if it exists. ∎

Since the difference between $E_{11}I_a + E_{11}I_m$ and $E_{21}I_a + E_{21}I_m$ $\left(\text{i.e., } \frac{q\mu(\mu + d + \gamma + \epsilon)}{\beta_a(1 - q)(\mu + d + \gamma)}\right)$ with $\mu = \frac{1}{65 \times 365}$ is considerably small (0.0001619), then we select $\mu = 0.3$ and $I_c = 2.5$ while other parameters are defined in Table 2 in order to depict Case 1 clearly; i.e., $E_s \in \Omega \subset M$ achieves local asymptotic stability if (3.14) is fulfilled. Fig. 9 shows that any trajectory that begins either in region G_1 or G_2 will converge to $E_s \in \Omega \subset M$ if (3.14) is satisfied.

3.4.2. Case 2: E_{11} is a real equilibrium, whereas E_{21} is a virtual equilibrium

If the following constraint is satisfied, then E_{11} is a real equilibrium and E_{21} is a virtual equilibrium.

$$E_{11}I_a + E_{11}I_m < I_c \quad \text{and} \quad E_{21}I_a + E_{21}I_m < I_c. \tag{3.15}$$

Both E_{11}^R and E_{21}^V are located in region G_1. In this case, we have an equilibrium point located in G_1 (i.e., E_{11}) and there is no equilibrium point located in region G_2. If (3.15) is satisfied, then all trajectories in this case will converge to E_{11}^R. Hence, E_{11}^R achieves local asymptotic stability.

Theorem 3.8. E_{11}^R *is locally asymptotically stable if* (3.15) *is satisfied.*

(a) A trajectory with initial point in G_2 will hit and slide to the right on $\Omega \subset M$ before moving towards E_{11}^R.

(b) A trajectory will cross the region $S < h_1$ on M from the direction of G_2 before moving towards E_{11}^R.

(c) A trajectory that begins in region G_1 will converge to E_{11}^R without hitting or passing through manifold M.

(d) A trajectory will pass through M moving towards G_2 from G_1 and hit manifold M again from the direction of G_2. Then it will slide down on $\Omega \subset M$ before converging to E_{11}^R in G_1.
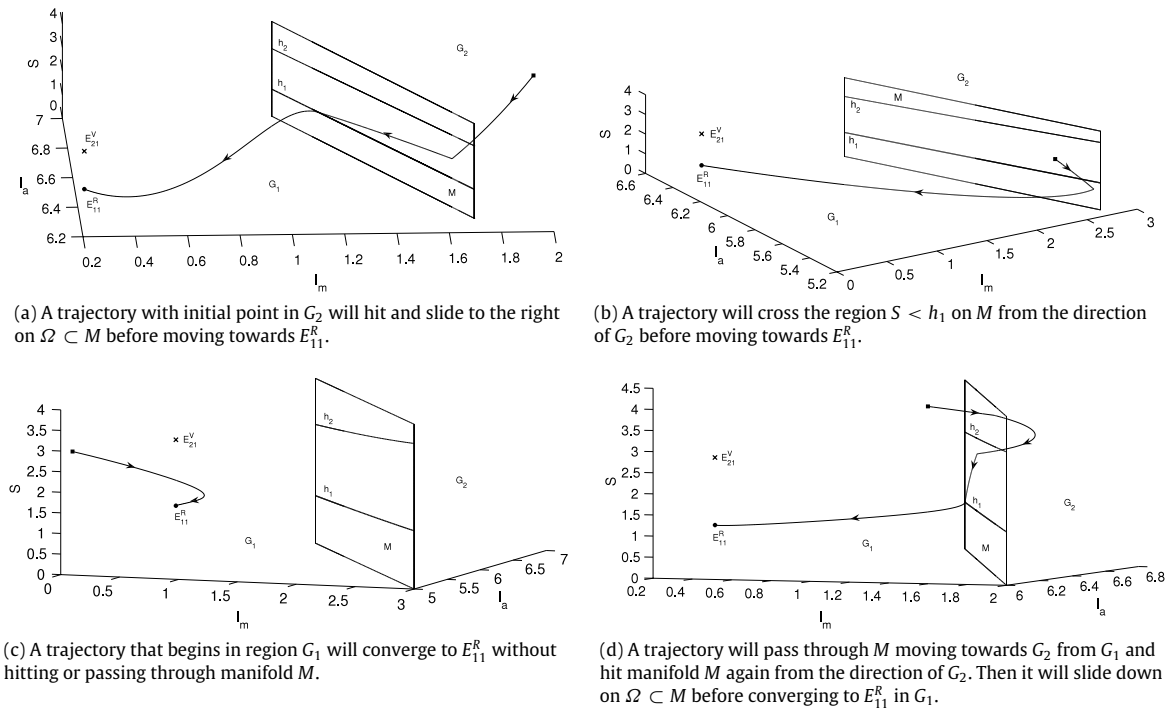
Fig. 10. $E_{11}^R \in G_1$ is locally asymptotically stable if (3.15) is fulfilled.

We discover that E_{11}^R is located in region G_1 if (3.15) is fulfilled. Since we have proved that the equilibrium point $E_{11} \in G_1$ achieves local asymptotic stability in Theorem 3.3, we omit the proof of Theorem 3.8.

Case 2 is depicted in Fig. 10 with $I_c = 8$. Any trajectory with initial point in region G_1 or G_2 will converge directly to E_{11}^R either without hitting the manifold M or it will hit the manifold M, slide and then move towards the equilibrium E_{11}^R.

3.4.3. Case 3: E_{21} is a real equilibrium, whereas E_{11} is a virtual equilibrium

E_{21} is a real equilibrium and E_{11} is a virtual equilibrium if (3.16) is satisfied.

$$E_{11}I_a + E_{11}I_m > I_c \quad \text{and} \quad E_{21}I_a + E_{21}I_m > I_c. \tag{3.16}$$

In this case, both E_{11}^V and E_{21}^R are located in region G_2. There is no equilibrium point that can be found in region G_1, but there is one equilibrium point (i.e., E_{21}) that lies in region G_2. All trajectories will converge to E_{21}^R if (3.16) is fulfilled. So E_{21}^R achieves local asymptotic stability in this case.

Theorem 3.9. E_{21}^R *achieves local asymptotic stability if the requirement of* (3.16) *is met.*

Note that E_{21}^R is located in region G_2 if (3.16) is satisfied. In Theorem 3.5, we have proved that the equilibrium point $E_{21} \in G_2$ is locally asymptotically stable. So we omit the proof of Theorem 3.9.

The result of Theorem 3.9 is illustrated in Fig. 11. All trajectories in this case with $I_c = 6$ will either hit or do not hit the manifold M before converging to E_{21}^R.

4. Conclusion and discussion

Two Filippov models that are governed by nonlinear ordinary differential equations with discontinuous right-hand sides have been proposed; notably the avian-only model with culling of infected birds and the SIIR model with quarantine as control measure. At the initial stage of an outbreak, many people are not aware of the existence of the disease. This usually leads to rapid disease outbreak since no disease preventions have been practiced by the public. When the emerging infectious disease has reached a critical stage, known as the "threshold level", people may start to take necessary precautions to prevent themselves from being infected [22]. Sliding mode control is one of the desirable methods to depict this type of disease-management phenomenon [21].

An HPAI outbreak in avian population can create havoc in the poultry industry; a large number of birds will have to be killed since culling birds is one of the primary strategy to eradicate an avian flu outbreak, especially among the infected avian population. Studies on culling have been carried out to identify the most effective approach to eradicating the disease
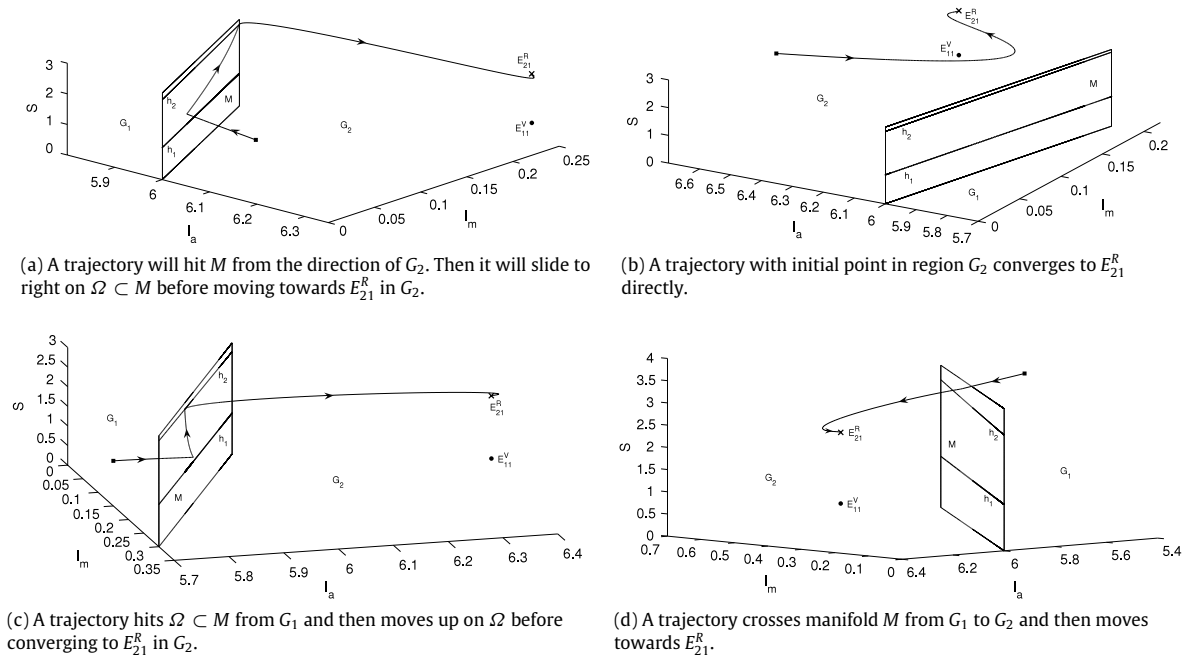
(a) A trajectory will hit M from the direction of G_2. Then it will slide to right on $\Omega \subset M$ before moving towards E_{21}^R in G_2.

(b) A trajectory with initial point in region G_2 converges to E_{21}^R directly.

(c) A trajectory hits $\Omega \subset M$ from G_1 and then moves up on Ω before converging to E_{21}^R in G_2.

(d) A trajectory crosses manifold M from G_1 to G_2 and then moves towards E_{21}^R.

Fig. 11. $E_{21}^R \in G_2$ is locally asymptotically stable if (3.16) is satisfied.

and reducing the socio-economic impact [16,45]. Hence it is essential for us to look closely at which culling threshold level should be chosen in order to eliminate the disease or at least to stabilize the infection. For instance, in the avian-only Filippov model (2.1), whenever the trajectory is found to be converging to E_{11d} in G_{1d} or $E_d \in \Omega_d \subset M_d$, we proclaim that the infection of avian influenza in the avian population is still bearable. However, if the solution of model (2.1) converges to E_{21d} in G_{2d}, we assume that an outbreak is emerging. As a response to the outbreak, control methods have to be implemented in order to suppress the transmission and contain the disease. In addition, the theoretical results and numerical simulations in Section 2 show that model (2.1) achieves global asymptotic stability.

Due to the influenza pandemic history, HPAI outbreaks, mainly H5N1, have caused severe infections in humans and resulted in many human deaths [46]. Many types of interventions have been applied to minimize the impact of avian influenza. Quarantine is one of the conventional control methods that has been widely used, especially in the absence of medicines and vaccines, during the onset of the outbreak to reduce the transmission rate of the disease. However, quarantine policy (e.g., location of quarantine, timeframe, who can set up quarantine, the use of legal orders and who has the authority to issue the orders and so on), limitations of resources (e.g., food, clean drinking water and medical equipments) and the lack of health-care workers are some of the most critical issues for public-health authorities [47,48]. Hence, an SIIR model with quarantine as a control measure is designed to assess an appropriate quarantine threshold level that will lead to disease elimination. In Section 3, it is shown that the solutions of model (3.1) will converge to either one of the two endemic equilibria or the sliding equilibrium. In order to inhibit an outbreak or to stabilize the infection, we have to choose a suitable tolerance threshold I_c such that the trajectory of model (3.1) is approaching E_{11} in G_1 or a sliding equilibrium E_s on $\Omega \subset M$.

There are several limitations of these two models that should be mentioned here. Throughout the model simulations, fixed constants of bird inflow and human recruitment have been applied in avian-only and SIIR models. We have made assumptions that the immunity of humans was permanent (i.e., recovered humans will not move to susceptible class) and the human-to-human transmission rate with avian strain is greater than the human-to-human transmission rate with mutant strain. For the avian population, infected birds are presumed to stay infected; i.e., infected birds will not move to other classes such as susceptible and recovered compartments. It is also noteworthy that we assumed humans with avian and mutant strains have the same values of recovery and additional disease death rate.

Our findings show that we can either preclude the influenza outbreak or stabilize the infection at a desired level by choosing an appropriate threshold level. A well-defined threshold policy is essential to us in order to combat an outbreak effectively and efficiently.

Acknowledgments

Appendix A. Types of regions on a discontinuity surface *M*

Suppose an ordinary differential equation

$$\dot{x} = f(x, t) \tag{A.1}$$

with threshold policy is discontinuous on a surface *M* that is defined by equation

$$\sigma(x) = 0$$

where $x \in \mathbb{R}^n$. The surface *M* separates the *x* space into domains G^- and G^+. Let us denote the differential equations that represent the dynamics in the regions G^- and G^+ as $f^-(x, t)$ and $f^+(x, t)$, respectively.

There are three types of regions on *M*: sliding, sewing and escaping regions [23], which are defined as follows.

Definition A.1 (*[23]*).

(a) If $\langle n, f^- \rangle > 0$ and $\langle n, f^+ \rangle < 0$ on $\Omega \subset M$, then Ω is known as a sliding region.
(b) If $\langle n, f^- \rangle \cdot \langle n, f^+ \rangle > 0$, i.e., $\langle n, f^- \rangle$ and $\langle n, f^+ \rangle$ have the same signs on $\Omega_2 \subset M$, then Ω_2 is called as a sewing region.
(c) If $\langle n, f^- \rangle < 0$ and $\langle n, f^+ \rangle > 0$ on $\Omega_3 \subset M$, then Ω_3 is known as an escaping region.

Note that escaping and sliding regions cannot exist simultaneously; it is impossible that $\langle n, f^- \rangle < 0$ and $\langle n, f^+ \rangle > 0$ exist at the same time with $\langle n, f^- \rangle > 0$ and $\langle n, f^+ \rangle < 0$.

Appendix B. Types of equilibrium points for a Filippov system

In this appendix, we will use similar notations as in Appendix A. Let us denote the sliding mode equation that describes the motion in the sliding region $\Omega \subset M$ by $f^0(x, t)$. Suppose there exists an equilibrium point in each region G^-, G^+ and Ω, denoted by E_1, E_2 and E_s, respectively. There are four types of equilibria that might exist in a model of ordinary differential equations with threshold policy: real, virtual, pseudoequilibrium and boundary equilibria [23].

Definition B.1 (*[23]*).

(a) E^R is a real equilibrium if $f^-(E^R) = 0$ and $\sigma(E^R) < 0$ or $f^+(E^R) = 0$ and $\sigma(E^R) > 0$.
(b) E^V is a virtual equilibrium if $f^-(E^V) = 0$ and $\sigma(E^V) > 0$ or $f^+(E^V) = 0$ and $\sigma(E^V) < 0$.
(c) E^B is a boundary equilibrium if $f^-(E^B) = 0$ and $\sigma(E^B) = 0$ or $f^+(E^B) = 0$ and $\sigma(E^B) = 0$.
(d) E^P is a pseudoequilibrium if E^P is an equilibrium point on the sliding mode; i.e., $f^0(E^P) = 0$ and $\sigma(E^P) = 0$.

Note that a stable virtual equilibrium will not be achieved as the dynamics will change once the trajectory hits the discontinuous manifold [23].

Appendix C. Lyapunov function and theories on global stability of the Filippov system

Consider a differential equation (A.1) with $f \in C^1(G)$ where *G* is an open subset of $\mathbb{R}^n$. The solution $\phi(t, x_0)$ of the initial-value problem (A.1) with $x_0 \in G$ will be a dynamical system on *G* if and only if $\forall x_0 \in G$, $\phi(t, x_0)$ is defined $\forall t \in \mathbb{R}$. The function $\phi(\cdot, x) : \mathbb{R} \to G$ for $x \in G$ defines a solution curve, trajectory or orbit of (A.1) with initial point $x_0 \in G$. A trajectory with $x_0 \in G$ can be described as a motion along the curve $\Gamma = \{x \in G; x = \phi(t, x_0), t \in \mathbb{R}\}$, which is defined by (A.1) (refer to [49] for further details).

Definition C.1 (*[49]*). A point $E \in G$ is an ω-limit point of the trajectory $\phi(\cdot, x)$ of (A.1) if there is a sequence $t_n \to \infty$ such that $\lim_{n \to \infty} \phi(t_n, x) = E$. The set of all ω-limit points of a trajectory Γ is called the ω-limit set of Γ and it is denoted by $\omega(\Gamma)$.

Definition C.2 (*[49]*). Let *G* be an open subset of $\mathbb{R}^n$, $f \in C^1(G)$ and $\phi_t : G \to G$ be the flow of the differential equation (A.1) defined $\forall t \in \mathbb{R}$. Then a set $S \subset G$ is called invariant with respect to the flow ϕ_t if $\phi_t(S) \subset S \; \forall t \in \mathbb{R}$ and *S* is called positively invariant with respect to the flow ϕ_t if $\phi_t(S) \subset S \; \forall t \geq 0$.

Let $\Gamma_1(t) := \{x \in \mathbb{R}^n_+; x = \phi(t, x_0) \text{ for some } x_0 \in G\}$ and $\zeta(G) := \bigcup_{t \geq 0} \Gamma_1(t)$.

Definition C.3 (*[50,23]*). A function $V \in C^1(\mathbb{R}^n)$ is called a Lyapunov function of (A.1) on $G \subset \mathbb{R}^n$ if it is non-negative on *G* and, $\forall x \in G$,

$$\dot{V}^*(x) := \max_{\eta \in g(x)} \langle \nabla V(x), \eta \rangle \leq 0 \quad \text{where}$$

$$g(x) := \begin{cases} f^-(x); & x \in G^- \\ \alpha f^+(x) + (1 - \alpha)f^-(x); & x \in M \text{ where } \alpha \in [0, 1] \\ f^+(x); & x \in G^+. \end{cases}$$

Proposition C.1 (*[50,23, LaSalle's Invariance Principle]*)**.** *Suppose $G \subset \mathbb{R}^n$ is an open set that satisfies $\omega(G) := \bigcup_{x \in G} \omega(x) \subset \zeta(G)$. Let every Filippov solution $\phi(t, x_0)$ of (A.1) be unique and defined $\forall t \geq 0$ and $x_0 \in G$. Suppose $V : \mathbb{R}^n \to \mathbb{R}$ is a Lyapunov function of (A.1) on $\zeta(G)$. Then $\omega(G)$ is a subset of the largest positively invariant subset of $\overline{\Sigma}$ where $\Sigma := \{x \in \overline{G}; \dot{V}^*(x) = 0\}$.*

Corollary C.2 (*[50,23]*)**.** *Assume that G and $V : \mathbb{R}^n \to \mathbb{R}$ satisfy Proposition C.1 and $\mathbb{R}^n \setminus G$ is repelling in the sense that all solutions stay in $\mathbb{R}^n \setminus G$ for only a finite time. Let $\omega(\mathbb{R}^n) = \omega(G)$ be bounded. Then $\overline{\omega(\mathbb{R}^n)}$ is globally asymptotically stable.*

Theorem C.3 (*[49, Dulac's Theorem]*)**.** *Suppose*

$$\frac{dx}{dt} = f(x, y) \quad and \quad \frac{dy}{dt} = g(x, y) \tag{C.1}$$

where $f(x, y)$ and $g(x, y)$ are assumed to be C^1 functions. If there exists a C^1 function $B(x, y)$ (where $B(x, y)$ is also known as a Dulac function) in a simply connected region R such that $\frac{\partial(Bf)}{\partial x} + \frac{\partial(Bg)}{\partial y}$ has constant sign and is not identically zero in any subregion, then system (C.1) does not have a periodic orbit lying entirely in R.

References

[1] R. Goodwin, S. Sun, Public perceptions and reactions to H7N9 in Mainland China, J. Infect. 67 (2013) 458–462.
[2] World Health Organization. 2013. Human infection with influenza A (H7N9) virus in China-update. http://www.who.int/csr/don/2013_04_03/en/index.html (Accessed October 28, 2013).
[3] Centers for Disease Control and Prevention. 2013. Avian influenza A (H7N9) virus. http://www.cdc.gov/flu/avianflu/h7n9-virus.htm (Accessed October 30, 2013).
[4] Centers for Disease Control and Prevention. 2010. Key facts about avian influenza (bird flu) and highly pathogenic avian influenza A (H5N1) virus. http://www.cdc.gov/flu/avian/gen-info/facts.htm (Accessed October 30, 2013).
[5] World Health Organization. 2011. New: WHO comment on the importance of global monitoring of variant influenza viruses. http://www.who.int/influenza/human_animal_interface/avian_influenza/h5n1-2011_12_19/en/index.html (Accessed October 30, 2013).
[6] World Health Organization. 2012. H5N1 avian influenza: Timeline of major events. http://www.who.int/influenza/human_animal_interface/avian_influenza/H5N1_avian_influenza_update.pdf (Accessed October 30, 2013).
[7] D. Zilberman, J. Otte, D. Roland-Host, D. Pfeiffer, The cost of saving a statistical life: a case for influenza prevention and control, Nat. Resour. Manag. Policy 36 (2012) 135–141.
[8] F.B. Agusto, A.B. Gumel, Qualitative dynamics of lowly- and highly-pathogenic avian influenza strains, Math. Biosci. 243 (2013) 147–162.
[9] M.E. Alexander, S.M. Moghadas, J. Wu, A delay differential model for pandemic influenza with antiviral treatment, Bull. Math. Biol. 70 (2008) 382–397.
[10] T.C. Germann, K. Kadau, I.M. Longini, C.A. Macken, Mitigation strategies for pandemic influenza in the United States, Proc. Natl. Acad. Sci. USA 103 (2006) 5935–5940.
[11] E. Jung, S. Iwami, Y. Takeuchi, T.-C. Jo, Optimal control strategy for prevention of avian influenza pandemic, J. Theoret. Biol. 260 (2009) 220–229.
[12] K.I. Kim, Z. Lin, L. Zhang, Avian-human influenza epidemic model with diffusion, Nonlinear Anal. RWA 11 (2010) 313–322.
[13] M. Lipsitch, T. Cohen, M. Murray, B.R. Levin, Antiviral resistance and the control of pandemic influenza, PLoS Med. 4 (2007) e15.
[14] N.M. Ferguson, D.A.T. Cummings, S. Cauchemez, C. Fraser, S. Riley, A. Meeyai, S. Iamsirithaworn, D.S. Burke, Strategies for containing an emerging influenza pandemic in Southeast Asia, Nature 437 (2005) 209–214.
[15] M. Nuño, G. Chowell, A.B. Gumel, Assessing the role of basic control measures, antivirals and vaccine in curtailing pandemic influenza: scenarios for the US, UK and the Netherlands, J. R. Soc. Interface 4 (2006) 505–521.
[16] H. Gulbudak, M. Martcheva, Forward hysteresis and backward bifurcation caused by culling in an avian influenza model, Math. Biosci. (2013) http://dx.doi.org/10.1016/j.mbs.2013.09.001.
[17] F.B. Agusto, Optimal isolation control strategies and cost-effectiveness analysis of a two-strain avian influenza model, Biosystems 113 (2013) 155–164.
[18] N.S. Chong, J.M. Tchuenche, R.J. Smith?, A mathematical model of avian influenza with half-saturated incidence, Theory Biosci. 133 (2014) 23–38.
[19] S. Tang, Y. Xiao, N. Wang, H. Wu, Piecewise HIV virus dynamic model with CD4$^+$ T cell count-guided therapy: I, J. Theoret. Biol. 308 (2012) 123–134.
[20] A. Wang, Y. Xiao, A Filippov system describing media effects on the spread of infectious diseases, Nonlinear Anal. Hybrid Syst. 11 (2014) 84–97.
[21] Y. Xiao, T. Zhao, Dynamics of an infectious diseases with media/psychology induced non-smooth incidence, Math. Biosci. Eng. 10 (2) (2013) 445–461.
[22] Y. Xiao, X. Xu, S. Tang, Sliding mode control of outbreaks of emerging infectious diseases, Bull. Math. Biol. 74 (2012) 2403–2422.
[23] T. Zhao, Y. Xiao, R.J. Smith?, Non-smooth plant disease models with economic thresholds, Math. Biosci. 241 (2013) 34–48.
[24] G. Matei, M. Decun, G.H. Ontanu, A comparative risk consequences assessment for avian influenza outbreaks occurred in Romania, Lucr. Ştiinţ. Med. Vet. XI (2007) 10–15.
[25] G. Sun, H. Yang, A study on the space–time dynamic of global avian influenza and relationship with bird migration, Int. J. Bus. Manag. 3 (2) (2008) 10–17.
[26] The Center for Food Security and Public Health. 2013. High pathogenicity avian influenza. http://www.cfsph.iastate.edu/DiseaseInfo/notes/AvianInfluenza.pdf (Accessed October 30, 2013).
[27] M. Koopmans, B. Wilbrink, M. Conyn, G. Natrop, et al., Transmission of H7N7 avian influenza A virus to human beings during a large outbreak in commercial poultry farms in the Netherlands, Lancet 363 (2004) 587–593.
[28] World Health Organization. 2010. Reducing the risk of emergence of pandemic influenza. http://www.who.int/influenza/resources/research/research_agenda_influenza_stream_1_reducing_risk.pdf (Accessed October 30, 2013).
[29] Food and Agriculture Organization of the United Nations. 2013. Poultry and human nutrition. http://www.fao.org/ag/againfo/themes/en/poultry/hh_nutrition.html (Accessed October 30, 2013).
[30] H.W. Hethcote, The mathematics of infectious diseases, SIAM Rev. 42 (4) (2000) 599–653.
[31] P. van den Driessche, J. Watmough, Reproduction numbers and sub-threshold endemic equilibria for compartmental models of disease transmission, Math. Biosci. 180 (2002) 29–48.
[32] J. Li, D. Blakeley, R.J. Smith?, The failure of R_0, Comput. Math. Methods Med. 2011 (2011) Article ID 527610.
[33] A.F. Filippov, Differential Equations with Discontinuous Right-hand Sides, Kluwer Academic, Dordrecht, The Nertherlands, 1988.
[34] R.I. Leine, Bifurcations in discontinuous mechanical systems of Filippov-type. The Universiteitsdrukkerij TU Eindhoven, The Netherlands, 2000.
[35] M. Martcheva, Avian flu: modeling and implications for control. AMS Subject Classification: 92D30, 92D40, 2011.
[36] N. Tuncer, M. Martcheva, Modeling seasonality in avian influenza H5N1, J. Biol. Syst. 21 (2013) Article ID 1340004.
[37] A.B. Gumel, Global dynamics of a two-strain avian influenza model, Int. J. Comput. Math. 86 (2009) 85–108.
[38] World Health Organization. 2013. Frequently asked questions on human infection caused by the avian influenza A (H7N9) virus. http://www.who.int/influenza/human_animal_interface/faq_H7N9/en/ (Accessed October 28, 2013).

[39] World Health Organization. 2013. Influenza at the human-animal interface. http://www.who.int/influenza/human_animal_interface/Influenza_Summary_IRA_HA_interface_7October13.pdf (Accessed October 28, 2013).
[40] World Health Organization. Avian influenza: food safety issues. http://www.who.int/foodsafety/micro/avian/en/index1.html (Accessed October 28, 2013).
[41] J. Lucchetti, M. Roy, M. Martcheva, A dynamic avian flu model and its fit to human avian influenza cases, in: J.M. Tchuenche, Z. Mukandavire (Eds.), Advances in Disease Epidemiology, Nova Science Publishers, New York, 2009, pp. 1–30.
[42] X. Yang, Generalized form of Routh–Hurwitz criterion and Hopf bifurcation of higher order, J. Appl. Math. Lett. 15 (2001) 615–621.
[43] V.I. Utkin, Sliding Modes in Control and Optimization, Springer-Verlag, Berlin, Heidelberg, 1992.
[44] J. Yang, S. Tang, R.A. Cheke, Global stability and sliding bifurcations of a non-smooth Gause predator–prey system, J. Appl. Math. Comput. 224 (2001) 9–20.
[45] A. Le Menach, E. Vergu, R.F. Grais, D.L. Smith, A. Flahault, Key strategies for reducing spread of avian influenza among commercial poultry holdings: lessons for transmission to humans, Proc. R. Soc. B 273 (2006) 2467–2475.
[46] World Health Organization. 2011. Avian influenza. http://www.who.int/mediacentre/factsheets/avian_influenza/en/ (Accessed November 5, 2013).
[47] National Association of County and City health Officials. 2006. Issues to consider isolation and quarantine. http://www.naccho.org/toolbox/_toolbox/IssuestoConsiderIsolation&Quarantine.pdf.
[48] North Country Regional Public Health Emergency Annex. 2011. Appendix 6—Isolation and quarantine. http://www.nchcnh.org/images/NCHCuplds/files/Appendix%206%20Isolation%20&%20Quarantine%20v4_0.pdf.
[49] L. Perko, Differential Equations and Dynamical Systems, third ed., Springer-Verlag, New York, 2001.
[50] D.S. Boukal, V. Křivan, Lyapunov functions for Lotka–Volterra predator–prey models with optimal foraging behavior, Math. Biol. 39 (1999) 493–517.